Sushil Ghimire

Candidate

Civil Engineering

Department

This thesis is approved, and it is acceptable in quality and form for publication:

Approved by the Thesis Committee:

Dr. Walter Gerstle , Chairperson

Dr. Fernando Moreu

Dr. Majeed Hayat

STUDY OF VIBRATION FOR DETECTION AND RECOGNITION OF CONCEALED MACHINERY WITHIN BUILDINGS

by

SUSHIL GHIMIRE

BACHELOR'S DEGREE IN CIVIL ENGINEERING
TRIBHUVAN UNIVERSITY, NEPAL

THESIS

Submitted in Partial Fulfillment of the
Requirements for the Degree of

Master of Science
Civil Engineering

The University of New Mexico
Albuquerque, New Mexico

March, 2017

Dedication

To my father and mother Ambika Prasad Ghimire and Durga Kumari Koirala Ghimire, my brother, Ashish Ghimire, my advisor Dr. Walter Gerstle, and my beloved friend, Bidyah Dahal,

for their encouragement and support.

Acknowledgements

I am heartily thankful to Dr. Walter Gerstle, my advisor and committee chair, for giving me opportunity to work with him. This research is possible because of his continuous support, guidance, and encouragement.

I am thankful to the funding agency. This work is supported by the United States Department of Energy, Award No. DE-NA0002484.

I am extremely thankful to my parents for their encouragement and undoubted confidence in me.

I would like to thank Dr. Majeed Hayat and Dr. Fernando Moreu for being in my thesis committee member and Dr. Thomas Paez for reviewing my thesis.

I would also like to thank my colleagues, Francisco Pérez, Krishna Chaitanya Jagadeesh, and Jose Alberto Gomez for their help and support.

STUDY OF VIBRATION FOR DETECTION AND RECOGNITION OF CONCEALED MACHINERY WITHIN BUILDINGS

by

Sushil Ghimire

B.S., CIVIL ENGINEERING, TRIBHUVAN UNIVERSITY, NEPAL, 2014

M.S., CIVIL ENGINEERING, UNIVERSITY OF NEW MEXICO, USA, 2017

ABSTRACT

Recently international concern about nuclear proliferation has rapidly increased. Some governmental agencies have an interest in remotely detecting and recognizing concealed machinery within buildings to detect any anomalous activity occurring inside the building.

The vibration studies of the roof and the exhaust structures of an existing utility building, the Ford Utility Center at the University of New Mexico and a simplified laboratory structure representing an industrial building, called the doghouse are presented in this thesis. The vibration studies presented allow the reader to understand to what extent it is possible to identify machines concealed within a building.

To identify machines concealed within a complex building like the Ford Utility Center, we preferred first to better understand the vibration of a simplified structure due to concealed machinery. Thus, in this thesis, we first study the vibration of the doghouse, and then study the vibration of the Ford Utility Center.

Table of Contents

List of Figures ..... **ix**

List of Tables ..... **xiv**

Chapter 1 Introduction **1**

1.1. Motivation 1

1.2. Scope of thesis 2

1.3. Outline of thesis 3

Chapter 2 Literature Review **5**

2.1. Introduction 5

2.2. Vibration measurement and analysis 6

2.3. Identification of concealed machinery by vibrations 6

2.4. Nonlinearity in structural vibration 8

2.5. Displacement time history of vibration 9

2.6. Summary 10

Chapter 3 Data Acquisition Process and Sensitivity of Accelerometer **12**

3.1. Introduction to the data acquisition process 12

3.2. Components of data acquisition process 13

3.3. Sensitivity of the accelerometer 15

3.4. Summary 20

Chapter 4 Displacement Reconstruction from Measured Acceleration **22**

4.1. Introduction 22

4.2. Time domain method of displacement reconstruction 23
4.3. Error using the time domain method 25
4.4. Frequency domain method of displacement reconstruction 28
4.5. Introduction of high pass filter 31
4.6. Summary 33

Chapter 5 Free Vibration Study of the Doghouse 34

5.1. Introduction 34
5.2. Description of the laboratory structure 36
5.3. Finite element analysis 41
5.4. Experimental analysis 44
5.5. Summary 47

Chapter 6 Refined Vibrational Models of the Doghouse 49

6.1. Introduction 49
6.2. Nonlinearity 50
6.3. Nonlinearity based on the deformations of an elastic plate 52
6.4. Laboratory tests of the doghouse 53
6.5. Finite element analysis of the doghouse 59
6.6. Summary 64

Chapter 7 Identification of Motors Concealed within the Doghouse 66

7.1. Introduction 66
7.2. Linear dynamics 67
7.3. Linear forced vibration analysis 69
7.4. Laboratory tests of the doghouse 74

7.5. Summary 77

Chapter 8 Vibration Study of the Ford Utility Center 78

8.1. Introduction 78

8.2. Ford Utility Center 79

8.3. Vibration signatures of the roof 82

8.4. Summary 87

Chapter 9 Conclusions 88

9.1. Summary 88

9.2. Major findings 89

9.3. Future research 90

References 92

List of Figures

Fig. 2.1. a) Top hat chimney reflector. b) Top view of the chimney, with C 4x6.25 channel weights and a motor with off balance mass shown (Pérez, Campbell et al. 2016). 7

Fig. 3.1. Schematic of our data acquisition process using national instruments hardware NI- DAQ) and Software (LabVIEW)..... 12

Fig. 3.2. Functional diagram of piezo-electric accelerometer 13

Fig. 3.3. Experimental setup with two accelerometers and a hydraulic actuator..... 16

Fig. 3.4. Time history and magnitude spectrum of the hydraulic actuator measured by accelerometer1 17

Fig. 3.5. Magnified picture of Fig. 3.4. 18

Fig. 3.6. Time history and magnitude spectrum of the hydraulic actuator measured by accelerometer2. 19

Fig. 3.7. Magnified picture of Fig. 3.6. 20

Fig. 4.1. Time history of reconstructed velocity and displacement from acceleration measured on the hydraulic actuator using time domain method of reconstruction. . 24

Fig. 4.2. Time history of reconstructed velocity and displacement from acceleration measured on the chimney using time domain method of reconstruction. 24

Fig. 4.3. Time history of sinusoidal waveform of unit amplitude and frequency of 2 Hz and its integrated waveform. 26

Fig. 4.4. Time history of sinusoidal waveform of unit magnitude and frequency of 20 Hz and its integrated waveform. 26

Fig. 4.5. Time history of multi frequency sinusoid and its integrated waveform. 27
Fig. 4.6. Time history of reconstructed displacement from acceleration measured on the hydraulic actuator using frequency domain method. 30
Fig. 4.7. Time history of reconstructed displacement from acceleration measured on the chimney actuator using frequency domain method. 30
Fig. 4.8. Fourier transform of acceleration time history of the chimney. 31
Fig. 4.9. Reconstructed displacement of chimney using high pass filter on frequency domain method. 32
Fig. 5.1. Damped spring-mass-system. 34
Fig. 5.2. Construction drawings of the doghouse. 37
Fig. 5.3. Construction drawings of the doghouse. 38
Fig. 5.4 Construction drawings of the doghouse. 39
Fig. 5.5. Doghouse. 40
Fig. 5.6. Connection of chimney with roof and walls. Front wall removed. 40
Fig. 5.7 Finite element model of the doghouse using SAP2000. 41
Fig. 5.8. First mode of vibration of the doghouse using SAP2000. 43
Fig. 5.9. Second mode of vibration of the doghouse using SAP 2000. 43
Fig. 5.10. Experimental setup to measure free vibration of the chimney. 44
Fig. 5.11. Damped free vibration time history, and magnitude spectrum of chimney of the doghouse, measured by the accelerometer. 45
Fig. 5.12. Experimental setup to measure the free vibration of the roof. 46
Fig. 5.13. Damped free vibration time history and magnitude spectrum of roof of the doghouse, measured by accelerometer. 47

Fig. 6.1. Doghouse after removal of the chimney and hole in the roof. 50

Fig. 6.2. Experimental setup to measure free vibration of the roof with an accelerometer. 54

Fig. 6.3. Time history and magnitude spectrum of vibration of the roof for connection type A. 55

Fig. 6.4. Time history and magnitude spectrum of vibration of the roof for connection type B. 56

Fig. 6.5. Time history and magnitude spectrum of vibration of the roof for connection type C. 56

Fig. 6.6. Experimental setup to measure damped free vibration at the center of the long sidewall using an accelerometer. 57

Fig. 6.7. Time history and magnitude spectrum of vibration of the long sidewall for connection type A. 58

Fig. 6.8. Time history and magnitude spectrum of vibration of the long sidewall for connection type B. 58

Fig. 6.9. Time history and magnitude spectrum of vibration of the long sidewall for connection type C. 59

Fig. 6.10. Fundamental mode of vibration (10.36Hz) of the doghouse with connection type C using SAP2000. 60

Fig. 6.11. a) Linear static analysis of the doghouse under the gravity load, and b) Nonlinear static analysis of the doghouse under the gravity load for connection type C. 61

Fig. 6.12. a) Fundamental mode shape and frequency of the long sidewall and b) Fundamental mode shape and frequency of the roof for connection type C, using stress stiffened modes. 62
Fig. 6.13. a) Fundamental mode shape and frequency of the long sidewall and b) Fundamental mode shape and frequency of the roof for connection type A, using stress stiffened modes. 63
Fig. 6.14. a) Fundamental mode shape and frequency of the long sidewall and b) Fundamental mode shape and frequency of the roof for connection type B, using stress-stiffened modes. 64
Fig. 7.1. Damped spring mass system. 69
Fig. 7.2. Time history and magnitude spectrum of the input waveform measured in laboratory used for the time history simulation. 72
Fig. 7.3. SAP2000 model of the doghouse with the applied force to perform time history analysis. 72
Fig. 7.4. Displacement time history and frequency output at the top of the chimney obtained from linear time history analysis for an input from Fig. 7.2. 73
Fig. 7.5. Picture showing two motors firmly attached with the connecting plates and concealed within the doghouse. 74
Fig. 7.6. Time history and magnitude spectrum recorded at the chimney when only Motor 1 is turned on. 75
Fig. 7.7. Time history and magnitude spectrum recorded at the chimney when only Motor 2 is turned on. 76

Fig. 7.8. Time history and magnitude spectrum recorded at the chimney when both motors are turned on. 76
Fig. 8.1. Site plan of Ford Utility Center. 79
Fig. 8.2. First floor plan of Ford Utility Center. 80
Fig. 8.3. Equipment layout of Ford Utility Center. 81
Fig. 8.4. Picture of two Cogeneration plants within Ford Utility Center. 82
Fig. 8.5. Google image of the roof of Ford Utility Center. 83
Fig. 8.6. Magnitude spectra of the vibrations measured at Location 1 on three dates. 85
Fig. 8.7. Magnitude spectra of the vibrations measured at the Location 2 on three dates. 86

List of Tables

Table. 5.1. Fundamental frequency of the doghouse predicted by SAP2000 and experiment..... 48

Table. 6.1. Comparison between fundamental frequencies of the long sidewall and the roof predicted by linear and nonlinear finite element approach (SAP2000) and experimental tests..... 65

Table. 8.1. Machinery operating in the Ford Utility Center on the given three dates. 84

Chapter 1 Introduction

1.1. Motivation

We live in the age of science and technology. Engineers and scientists are proposing new inventions almost every day to make human life convenient. For example, bridges, spacecraft, electronics, better medical treatment, and luxuries are all brought by scientific advancement. However, scientific advancement has also created harm. It has created greater threats like guns and bombs that world would have been a better place without.

Many countries are trying to develop nuclear weapons, thus there is a great threat of nuclear holocaust in future world wars. A nuclear holocaust is a scenario involving widespread destruction and radioactive fallout causing the collapse of civilization, through the use of nuclear weapons. Recently, international concern about nuclear proliferation has rapidly increased.

Some governmental agencies have an interest in remotely detecting and recognizing concealed machinery within buildings to detect any anomalous activity occurring inside the building. It is known that vibrating machines concealed within buildings produce vibration of the building envelope. As many of these signatures can be correlated to the machinery concealed within the building, agencies may be able to reliably detect nuclear proliferation missions at particular sites of interest. Therefore, the motivation for this thesis is to answer the question: “By measuring the vibration signatures on the roof of a building, is it possible to identify the machine causing the vibration?”.

1.2. Scope of thesis

The Electrical and Computer Engineering Department and the Civil Engineering Department at the University of New Mexico are collaborating on the research project on remote detection and recognition of concealed machinery within a building using a vibration estimation and imaging approach using Synthetic Aperture Radar (SAR). This research project has been awarded by the United States Department of Energy and this thesis is written as part of this collaborative research project.

The purpose of this thesis is to study whether we can identify the types and locations of machines concealed within buildings using vibrational information obtained from the building envelopes. For the purpose of our study the Ford Utility Center at the University of New Mexico, which generates around 13 MW of electricity, hot and chilled water using natural gas has been selected. To assess a complex building like the Ford Utility Center, we needed first to better understand the theory of structural vibrations. To this end, we first studied the vibration of a simplified laboratory model representing an industrial building. Thus, a simplified model was built in the laboratory, representing a simplified industrial building which we call the “doghouse”.

Thus, this thesis first presents, a finite element and an experimental study of the vibration of the doghouse, and finally present a study of the Ford Utility Building to answer our primary question: “By measuring the vibration signatures on the roof of a building, is it possible to identify the machine causing the vibration?”.

Although the research project proposed to use Synthetic Aperture Radar (SAR) for vibration estimation, the research team decided to use an accelerometer to record the vibration and then perform a flight test using SAR. The flight test was performed in the desert of Borrego Springs in California to record the vibration of the doghouse due to

concealed motors. However, the data recorded from SAR study is not presented in this thesis. Thus, all the vibration data presented in this thesis is obtained by an accelerometer.

1.3. Outline of thesis

This thesis includes nine chapters: Introduction, Literature Review, Data Acquisition Process and Sensitivity of Accelerometer, Displacement Reconstruction from Measured Acceleration, Free Vibration Study of the Doghouse, Refined Vibrational Models of the Doghouse, Identification of Motors Concealed within the Doghouse, Vibration Study of the Ford Utility Building, and Conclusions.

Chapter 2 provides a literature review of all material researched and relevant to this thesis. This chapter also provides the brief introduction to the previous research performed by a former graduate student from the University of New Mexico who worked on a similar research project.

Chapter 3 focuses on the data acquisition process we used throughout this thesis. In this chapter we provide the introduction to all the components of the data acquisition process and perform laboratory experiments to verify the accelerometer calibration factor provided by the data sheet provided with the accelerometer.

Chapter 4 presents the time domain and frequency domain methods to convert the acceleration signals into displacement signals. We will find that the frequency domain method is helpful in analyzing vibration signals. However, the frequency domain method still is not completely definitive.

Chapter 5 uses the linear elastic finite element method and the experimental tests to determine the vibrational characteristics of the doghouse. By comparing the finite

element results and the experimental results we will find that the linear finite element model is inadequate to accurately model the vibration behavior of the doghouse.

Chapter 6 discusses a nonlinear finite element method to model the effect of stress stiffening on vibration of the doghouse, and makes the case that this approach is more accurate than the linear finite element method. This chapter also discusses the effect of connections on the vibration of the doghouse.

Chapter 7 presents finite element analysis and experimental tests to study the relationship between periodic input force and periodic output response of the doghouse. This chapter investigates the possibility of predicting the vibration signatures of the chimney of the doghouse caused by two motors operating in it.

Chapter 8 discusses the possibility of correlating the vibration signatures obtained from the roof of the Ford Utility Center with the operation of the machines concealed in it.

Chapter 9 provides a brief summary of this thesis and also provides suggestions for future research work.

Chapter 2 Literature Review

This chapter's objectives are to:

- introduce the reader to some literature on identification of machinery from vibrations;
- provide the reader with some background in nonlinear plate vibrations;
- provide a brief introduction to displacement reconstruction from measured accelerations.

2.1. Introduction

In this chapter, we provide some background information on research conducted related to identification of concealed machinery using vibration measurement and analysis techniques. We first present some research on vibration measurement and analysis techniques and we find that vibrations measured from civil engineering infrastructure and rotating machines are mostly applied for the structural health monitoring purposes and for damage detection in machines. However, our context is a bit different: we want to perform vibration measurement and analysis to identify machinery concealed within a building. We present the review of a thesis written by a former civil engineering graduate student and a research paper published by team members of this research project.

Additionally, we present a brief review of literature related to nonlinear plate vibration theory and a brief review of displacement reconstruction from measured accelerations.

2.2. Vibration measurement and analysis

Vibration measurement and analysis techniques are becoming very popular in the industrial and research field for structural health monitoring purposes and to detect faults in rotating machinery like motors, pumps, turbines, and gearboxes. The basic idea is that the defects in the civil engineering structures and in rotating machines cause changes in vibrational response. Hence, damage and faults can be identified by examining the change in vibrational response of a structure (Chang, Flatau et al. 2003).

Vibration measurement are always done in the time domain using a variety of sensors; for example, accelerometers and strain gauges. The time history of recorded vibrations can be processed using the Fourier transform to obtain magnitude spectra. Frequencies thus obtained are used by many researchers to identify faulty components of structures (Doebling, Farrar et al. 1996) and (Farrar, Worden et al. 2007). However, we believe that these frequencies can also be related to the machines that are causing the enclosing structures to vibrate. My literature review found few attempts to use the vibrational frequencies obtained from a building envelope to identify the types and the locations of concealed machinery causing the vibration. In the next section, some of the work done by the former graduate students in this field of study are discussed.

2.3. Identification of concealed machinery by vibrations

Mareddy (2006) presented research on analyzing service level vibrations of a utility building to identify the type and location of concealed machinery within the building. The vibration data were collected from an existing utility building, the Ford Utility Center at the University of New Mexico. A finite element model of the Ford Utility Center was created using SAP2000 to provide a basis with which to compare the

observed vibrations. She compared the vibrations obtained from the roof of Ford Utility Center with the mode of vibrations from SAP2000 model to conclude her research. However, the Ford Utility Center is a complex two-story building and has many unknown details in it. The finite element model created by Mareddy had too many simplifying assumptions to be realistic, in my opinion.

Pérez, Campbell et al. (2016) performed research on the detection and estimation of vibrations generated by machinery concealed within a building and other structures. To this end, they performed a field test for three different vibrating targets, including one with a motor concealed inside a vibrating target. Fig. 2.1 shows the target used with a concealed motor in it.

a) b)

Fig. 2.1. a) Top hat chimney reflector. b) Top view of the chimney, with C 4x6.25 channel weights and a motor with off balance mass shown (Pérez, Campbell et al. 2016).

The top hat chimney reflector was actuated by a gear motor with an off-balance weight attached to it, as shown in Fig. 2.1a. A synthetic aperture radar (SAR) imaging from an airplane provided by General Atomics was used to acquire the vibrational data. The vibration data was simultaneously obtained using an accelerometer attached to the exterior surface of the chimney. Finally, by comparing the frequency of vibration data obtained from the accelerometer and SAR imaging technique, it was demonstrated that it is possible to capture the vibrational information of distant vibrating source using the SAR imaging technique. However, the use of this vibrational information to detect the operation of concealed machinery was left for the future research. The design of this structure was an attempt to imitate a chimney of an industrial building. The design is found to be unrealistic because, in most of all structure chimney, roof and the walls are coupled with each other. However, in this structure, the chimney was intentionally uncoupled with the roof, allowing the chimney to vibrate freely. This thesis is a continuation of the above-mentioned research.

2.4. Nonlinearity in structural vibration

Every real structure exhibits some degree of nonlinear behavior. Some structures are highly nonlinear and some are almost linear. Linearity is just an approximation to simplify an engineering problem; solutions obtained based on linear models are found to be adequate for many practical engineering purposes. However, the increased use of thin-walled structural components in the design of space vehicles, civil engineering infrastructure, and machinery and their vibrational behaviors at large amplitudes in response to the conditions they are subjected to, have recently attracted the attention of many investigators. As a result, the study of nonlinear flexural vibration of deformable

bodies, in particular plates, has received much attention in the literature (Sathyamoorthy 1987).

Engineers and scientists have developed theories on the geometrically nonlinear analysis of a plate. The Kirchhoff -Love theory of plates developed by (Love 1888) is a two dimensional mathematical model that is used to determine the stress and deformation in thin plates subjected to forces and moments. Von Karman later developed the geometrically nonlinear plate theory (Von Karman 1910). Recently, (Leissa 1969) published the theory on vibration of plates. There have been many different analytical methods developed to solve the nonlinear problem. However, by the survey of nonlinear detection and identification techniques for experimental vibrations (Allemang 1998) found that nonlinear structural dynamic system identification is often more a subjective art than it is a direct application of some particular method in systems theory. The nonlinear vibration problem is subjective because, although there are many analytical methods from which to choose, there is no general approach to detect, characterize, or model input-output relationships in nonlinear systems.

In this thesis, we find that the laboratory structure made up of steel plates show nonlinear behavior. Performing the nonlinear finite element analysis and experimental tests we identified the nonlinear behavior is mainly due to stress stiffening effect due to large deflection of the plate under its own weight. After taking the stiffening effect into account, the vibrations are essentially linear.

2.5. Displacement time history of vibration

Vibration measurement has become an important method in earthquake engineering, structural health monitoring, and damage detection. Vibration sensors are

able to measure vibration signals, enabled by the development of computer technology, electronic technology, and manufacturing processes. In this thesis, all the vibration signals are recorded by using an accelerometer. Although we are more interested on frequencies of measured vibrations, we also realized that, it is necessary also to know the displacement amplitude of the vibration.

It is possible to collect a displacement time history of a vibration using displacement sensors such as Linear Variable Differential Transducers (LVDTs). (Boothby, Domalik et al. 1998) and (Moreu, Jo et al. 2014) have used LVDT to measure the displacement time history of bridges for monitoring purposes. However, LVDTs require a fixed reference point from which to measure the displacement response, which is not practical in most cases. Hence, method for obtaining displacement time history from measured acceleration signals has gained much attention in the literature.

There has been much advance research on displacement reconstruction scheme using measured accelerations. (Lee, Hong et al. 2010) developed a method by formulating the reconstruction problem as a boundary value problem using a finite impulse filter and overlapping time window techniques to obtain the displacement signal from a measured acceleration. However, in this thesis, an attempt is made to obtain the displacement signal by performing the classical method of double integration of measured acceleration signal in the time domain and using DFT in the frequency domain.

2.6. Summary

We have outlined in this chapter research related to vibration measurement and analysis, nonlinearity in structural vibration, and displacement time history of vibration.

We find that most researchers have used the vibrational information obtained from bridges and buildings for damage detection and monitoring purpose. A former graduate student and a research team at the University of New Mexico have attempted to identify the operation of concealed machinery by using the vibrational information gleaned from the building envelope with some drawbacks and recommendations. This research overcomes some of the problems in the work performed by the former graduate student and research team. In this research first we replace the top hat chimney reflector used by (Pérez, Campbell et al. 2016) by a new laboratory structure called the "doghouse". We next perform finite element analysis and experimental tests on the doghouse to observe the relationship between the motors running inside the doghouse and the vibration signatures obtained on the roof of the doghouse. After gaining theoretical and experimental perspectives regarding the identification problem from a simple laboratory structure, we extend our study to more complex buildings such as, the Ford Utility Building to determine whether it is possible to identify the operation of machines concealed within the building by observing the vibration signatures on the roof of the building.

Chapter 3 Data Acquisition Process and Sensitivity of Accelerometer

This chapter's objectives are to:

- introduce the data acquisition process;
- describe the components of the data acquisition system;
- define and verify the accelerometer calibration factor.

3.1. Introduction to the data acquisition process

Data acquisition in structural dynamics is the process of recording the dynamic response of structures. Dynamic responses of the structure are acceleration, velocity, and displacement, among which acceleration is the easiest to measure.

Accurate data acquisition and processing are important in effective characterization and reliable evaluation of the structural system. For example, natural frequencies of various modes, damping ratios, and vibration signatures of forced vibration are identified based on experimentally obtained data, and the quality of these results is closely linked to the quality of the data obtained from the data acquisition system. To obtain high-quality data, a good understanding of the data acquisition process is important. Fig. 3.1 shows a schematic of our data acquisition process when using the National Instrument hardware (NI DAQ) and software (LabVIEW).

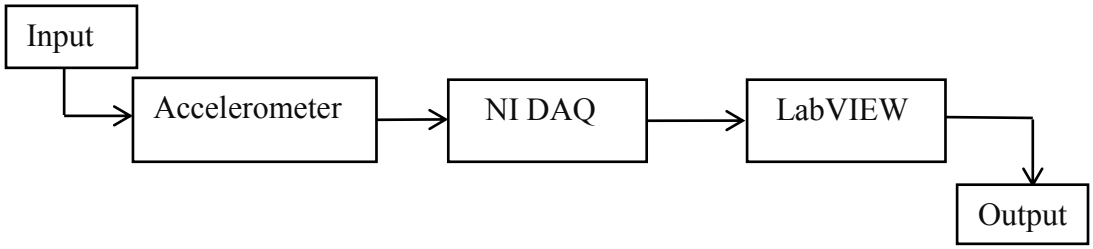

Fig. 3.1. Schematic of our data acquisition process using national instruments hardware NI-DAQ) and Software (LabVIEW)

3.2. Components of data acquisition process

Although most of the sensors used in structural systems are analog devices, data acquisition is usually performed with the digital computers. To be recorded on a computer, the analog signals must be discretized in the time and magnitude which is done by the various components of the data acquisition process, which is briefly described below.

With reference to Fig. 3.1, the input is mechanical acceleration caused by known or unknown forces in accordance with Newton's Laws of Motion.

3.2.1 Accelerometer

A transducer is defined generally as a device that converts one form of energy to another. An accelerometer is simply a transducer that converts mechanical acceleration into a proportional electrical signal. For our research, we are using the piezoelectric accelerometer, as shown in Fig. 3.2.

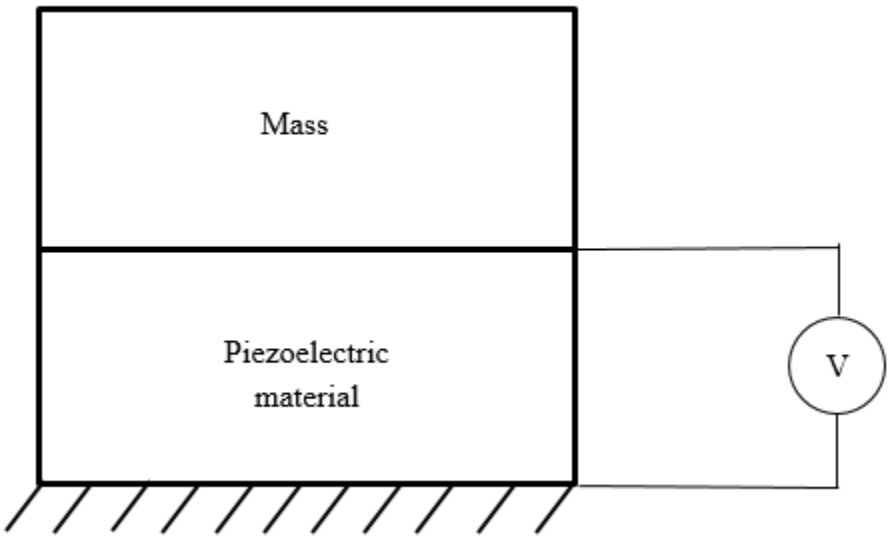

Fig. 3.2. Functional diagram of piezo-electric accelerometer

Piezo-electric crystals are man-made or naturally occurring crystals that produce an electric charge output when they are compressed, flexed or subjected to vibration. The word Piezo came from the Greek word 'Piezien' which means squeeze. In a piezo-electric accelerometer, a mass is attached to a piezo-electric crystal which is, in turn, mounted to the case of the accelerometer. When the case of the accelerometer is subjected to vibration the mass mounted on the crystal wants to stay still in space due to inertia and so compresses and stretches the piezo-electric crystal. This force causes a charge to be generated and due to Newton's 2nd law, F=ma, this force is proportional to acceleration. Thus, the accelerometer outputs an electrical voltage signal.

3.2.2 NI DAQ

The National Instruments Data Acquisition System, abbreviated by the acronym NI DAQ, samples analog signals that measure real world physical conditions and converts the resulting analog signals into digital numeric data that can be manipulated by a computer. The DAQ converts analog waveforms into digital values for processing.

Data acquisition applications are usually controlled by software programs developed using various general purpose programming languages such as C, C++, FORTRAN, LabVIEW etc. In our case we are using National Instrument DAQ model 9178 which provides input to LabVIEW.

The DAQ takes the continuous analog voltage input from the accelerometer and converts this into digital voltage output (bits).

3.2.3 LabVIEW

LabVIEW is software which reads output voltage signals from the DAQ and processes the signals to produce useful images and data. The DAQ here is connected by a Universal Serial Bus, USB. The USB serves as the communication interface between the DAQ device and LabVIEW for passing instructions and measured data. LabVIEW finally gives an output in the form of an ASCII file which can be read into MATLAB for further processing and visualization.

3.3. Sensitivity of the accelerometer

The Sensitivity of an accelerometer referred to as the "accelerometer calibration factor", is the ratio of the sensor's electrical output to mechanical input. The output we get from data acquisition process described above is in volts, but we need the acceleration in m/s^2. Using the accelerometer calibration factor, we can convert the voltage signal to meters per second squared (m/s^2).

According to the specification supplied with the accelerometer, the sensitivity of our model 353B52 by PCB PIEZOTRONICS is 51.0 $mV/(m/s^2)$. Hence, the accelerometer calibration factor is given by

In this chapter, we check this accelerometer calibration factor value given by the specification. An experiment is conducted to determine whether this value is accurate.

3.3.1 Equipment used in experiment

We seek to calibrate a PCB 353B52 accelerometer, hereafter called Accelerometer1. It is an accelerometer we are using for our research and trying to

confirm its calibration factor as given by its specification. We record data with a sampling frequency of 1650 samples/sec using our NI DAQ. Accelerometer1 is the left accelerometer shown in Fig. 3.3.

As a reference, we use a PCB 353B33 accelerometer, hereafter called Accelerometer2. It is an accelerometer which is already in use for research and calibrated. According to the specification supplied with the accelerometer, the sensitivity of this model is 100.5 mV/g. Data from this accelerometer is recorded with a sampling frequency of 1600 samples/sec using the DAQ. Accelerometer2 is the right accelerometer shown in Fig. 3.3.

We used a hydraulic actuator, as shown in Fig. 3.3, to excite both the accelerometers identically. The hydraulic actuator is a computer controlled system and can be operated with predefined frequency and displacement amplitude in the vertical direction.

Fig. 3.3. Experimental setup with two accelerometers and a hydraulic actuator.

3.3.2 Experimental procedure

Fig. 3.3. shows the experimental setup for measuring the vibration of the hydraulic actuator by two accelerometers. Accelerometer1 and Accelerometer 2 are attached on the bottom of the hydraulic actuator to record the vibration in a vertical direction. The hydraulic actuator is excited with a frequency of 2 Hz and displacement amplitude of 0.5 inches sinusoidally.

3.3.3 Observation

The vibration data of Accelerometer1 is converted to m/s^2 by using the accelerometer calibration factor. The data is processed with Discrete Fourier Transform in MATLAB to obtain the frequency and acceleration magnitude of the vibration as shown in Fig. 3.4.

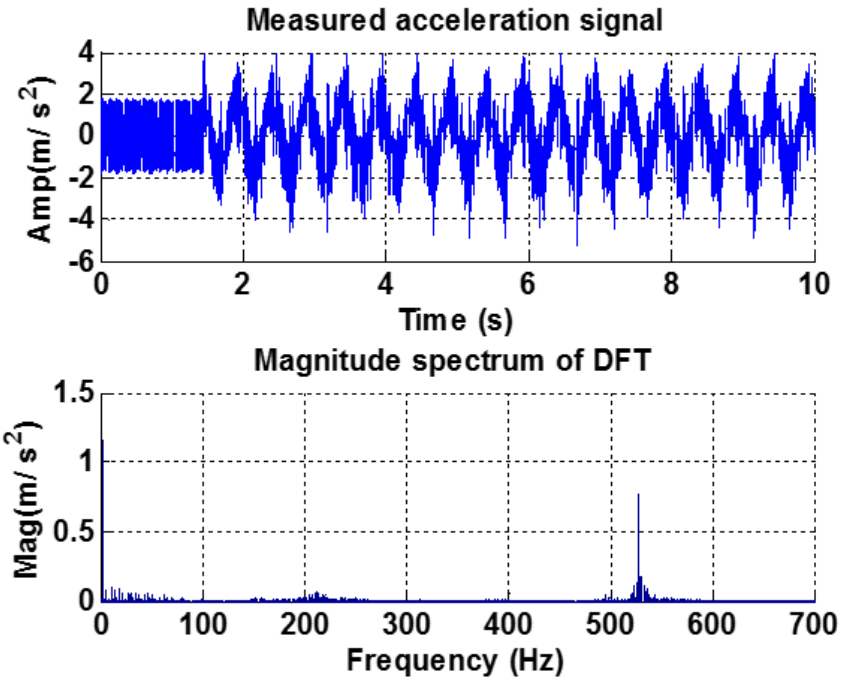

Fig. 3.4. Time history and magnitude spectrum of the hydraulic actuator measured by accelerometer1

In Fig. 3.4. we can see that there is a high-frequency signature of around 530 Hz. This experiment is conducted in the Structures Lab at the University of New Mexico with different kind of machines running simultaneously during the experiment. The noise created by these machines might be the cause for the high-frequency component. For this section, we are only interested in the low-frequency vibration of the hydraulic actuator, which is shown in Fig. 3.5.

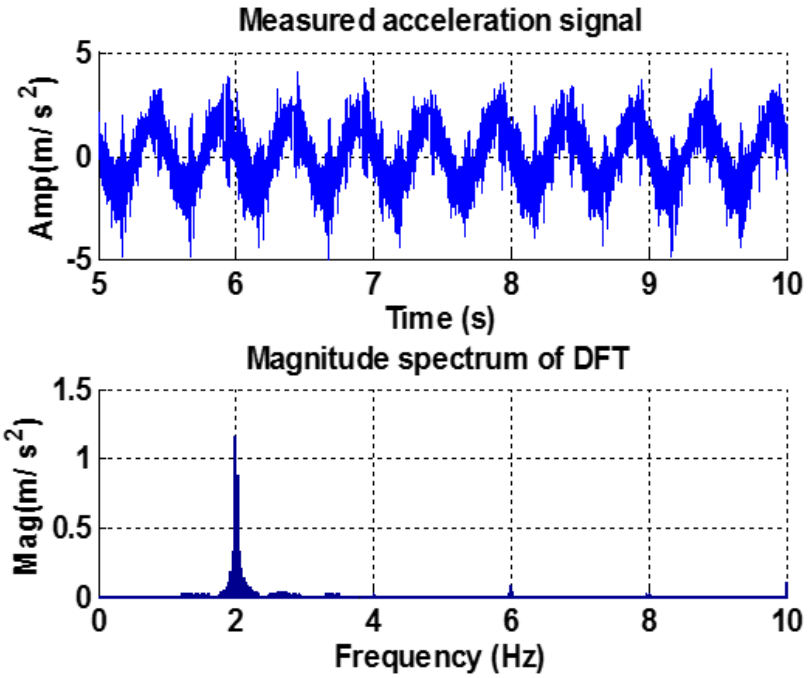

Fig. 3.5. Magnified picture of Fig. 3.4.

The frequency of vibration and the acceleration magnitude are found to be 1.99 Hz and 1.16 m/s^2 respectively.

The vibration data obtained from the Accelerometer2 is in m/s^2, which is processed with Discrete Fourier Transform in MATLAB to obtain the frequency and acceleration of the vibration, as shown in Fig. 3.6.

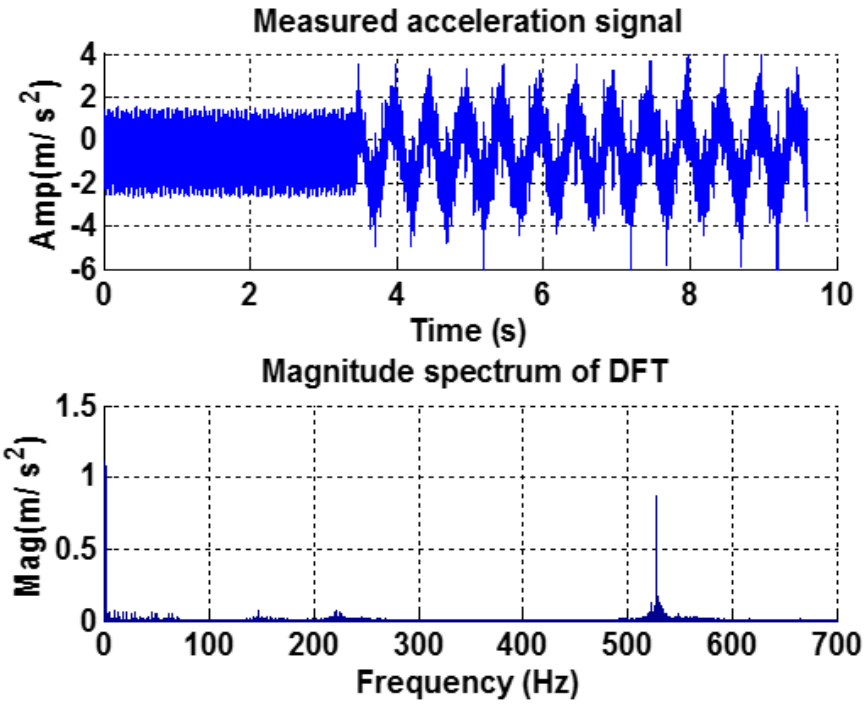

Fig. 3.6. Time history and magnitude spectrum of the hydraulic actuator measured by accelerometer2.

In Fig 3.6, we can see that there is a high-frequency signature of around 530 Hz. The most probable reason for this high-frequency component is already described above. Also in this section, we are interested in the low-frequency vibration of the hydraulic actuator, which is shown in Fig. 3.7.

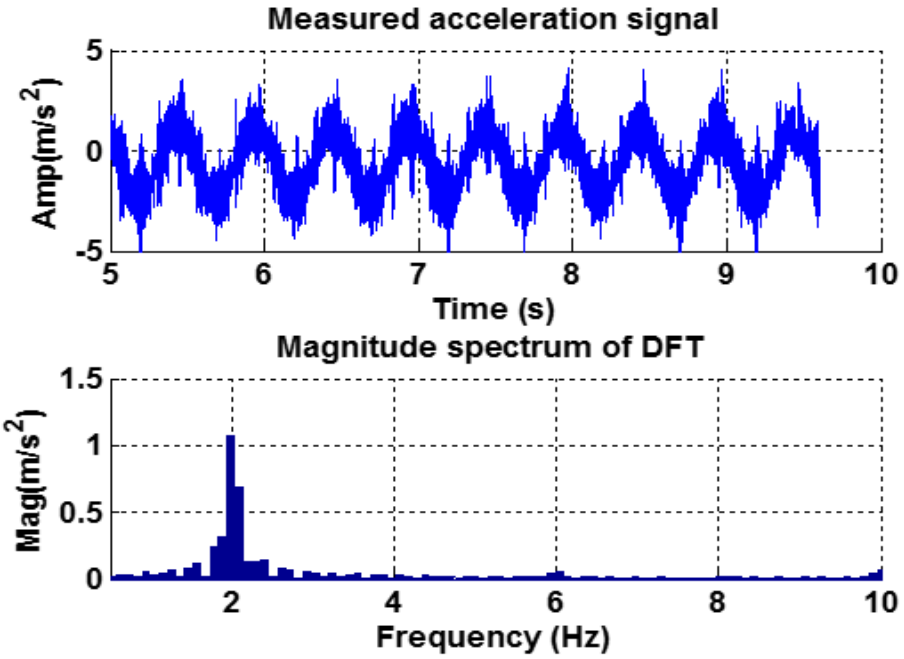

Fig. 3.7. Magnified picture of Fig. 3.6.

The frequency of vibration and the acceleration magnitude are found to be 1.98 Hz and 1.08 m/s^2 respectively.

3.4. Summary

The percentage difference in frequency and acceleration are given by

For the same source of vibration, both the accelerometers are giving almost the same acceleration and frequency values by using their respective sensitivity as provided by their specification. Moreover, the value of frequencies given by both the

accelerometers are same as the vibrating frequency of the hydraulic actuator, which is 2 Hz. Hence, the accelerometer calibration factor of Accelerometer1 provided by the specification can be accepted to use in further research.

Chapter 4 Displacement Reconstruction from Measured Acceleration

This chapter's objectives are to:

- introduce some background on displacement reconstruction;
- discuss time domain method of displacement reconstruction and its limitations;
- discuss frequency domain method of displacement reconstruction and its limitations;
- introduce a high pass filter.

4.1. Introduction

Acceleration, velocity and displacement are the dynamic responses of structural systems. Dynamic responses are measured for various purposes such as damage detection, modal analysis, structural health monitoring and structural control. The dynamic responses sought depends on the purpose of the task. For example, in the case of a structure experiencing a severe event such as a strong earthquake or a typhoon, a quick decision on the possibility of structural damage could be made based upon the maximum displacement of the structure.

Accelerometers are the most frequently used transducers to measure the vibration responses of structures. Various types of accelerometers are commercially available for a wide range of dynamic frequencies. In this research, we are using PCB 353B52 accelerometer as discussed in Chapter 1. Acceleration can be measured just by placing the accelerometer on the vibrating structure; on the other hand, it is not easy to directly measure the displacement of a structure because this requires a fixed reference point to

measure. Fixed reference points are rarely available to install displacement transducers. Moreover, the reference point as well as the structure move together during vibration, and thus the direct measurement of displacement becomes almost impossible in large structures like bridges and buildings. Thus, the reconstruction of displacement from the measured acceleration signal is an attractive alternative to the direct measurement of displacement. There are two main methods, for converting acceleration signals to displacement signals. One is directly integrating the acceleration signal in the time domain, and the other is using the Discrete Fourier Transform (Han and Chung 2002).

4.2. Time domain method of displacement reconstruction

The velocity signal can be obtained by directly integrating the acceleration signal in time domain using following definition. Similarly, the displacement signal is the integral of the velocity :

(3.1)

(3.2)

where and are the initial velocity and initial displacement respectively. In this section, we assume the initial and final conditions of velocity and displacement to be zero. However, we never have a continuous signal so the approximate solution can be found by using numerical integration techniques such as rectangular or trapezoidal integration.

Using the time domain method, Fig. 4.1 shows the time histories of reconstructed velocity and displacement from acceleration measured on the hydraulic actuator described in section 3.3.1 vibrating with an amplitude of 0.5 inches (0.0127 m) and 2 Hz

frequency. Similarly using the T-D method, Fig. 4.2. represents the time history of reconstructed velocity and displacement from acceleration measured at the chimney of the doghouse. The doghouse is a laboratory structure used for this research which will be described later.

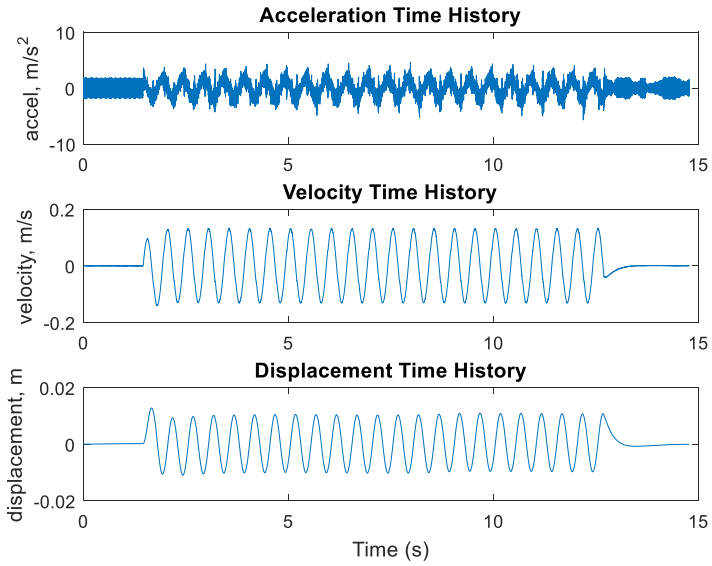

Fig. 4.1. Time history of reconstructed velocity and displacement from acceleration measured on the hydraulic actuator using time domain method of reconstruction.

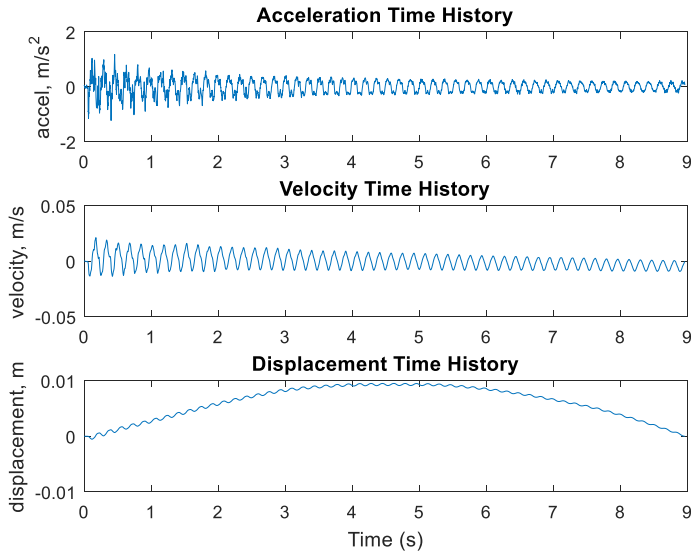

Fig. 4.2. Time history of reconstructed velocity and displacement from acceleration measured on the chimney using time domain method of reconstruction.

As can be observed, the reconstructed displacement of the hydraulic actuator seems quite reasonable. But, on the other hand the reconstructed displacement of the chimney seems implausible. There must be some error associated with this method of displacement reconstruction. We explore this error with examples in next section.

4.3. Error using the time domain method

As we have seen, most real data have multi frequency components. If the data contains even a small number of spurious low frequency components or a spurious constant Direct Current (DC or constant) offset, then the integrated time history will be incorrect. The unpredicted shape of integrated time history is due to these spurious components is in fact due to characteristic of integrated trigonometric functions that their amplitude increases with decreasing frequency, as discussed next.

4.3.1 Error due to spurious low frequency components

Let us consider a sinusoid of amplitude and cyclic frequency . This can be represented as

(3.3)

the indefinite integral of this waveform is given by

— (3.4)

where ‘ ’ is the constant of integration.

From these relations, we can see that the amplitude of the integrated component is inversely proportional to the frequency of the original signal. This can be shown by integrating the artificially created sinusoidal waveform in MATLAB. Fig. 4.3. represents

the sinusoidal waveform of unit amplitude and 2 Hz frequency and it's the integrated waveform.

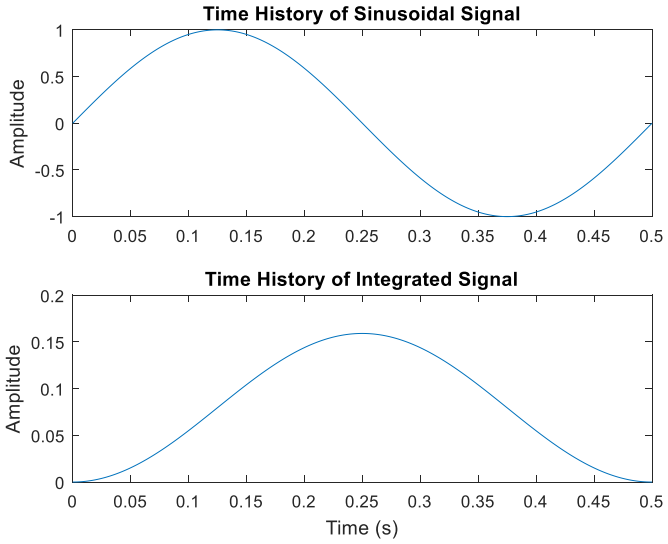

Fig. 4.3. Time history of sinusoidal waveform of unit amplitude and frequency of 2 Hz and its integrated waveform.

Fig. 4.4. represents the sinusoidal waveform of unit amplitude and 20 Hz frequency and it's the integrated waveform.

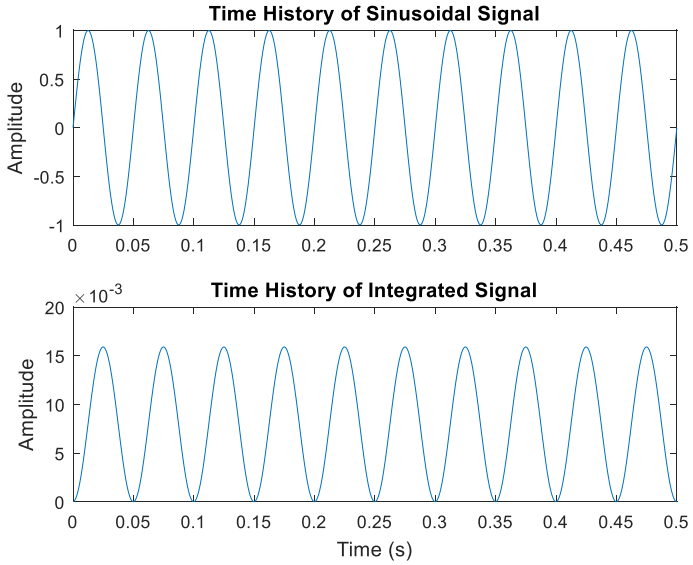

Fig. 4.4. Time history of sinusoidal waveform of unit magnitude and frequency of 20 Hz and its integrated waveform.

It is clear that the amplitude of the integrated waveform of 2 Hz frequency is 10 time higher than that of the 20 Hz waveform.

Let us add these two waveforms of same amplitude and frequencies of 2 Hz and 20 Hz to make a signal containing the two frequency components, represented as

(3.5)

where and are 2 Hz and 20 Hz respectively.

Fig. 4.5. represents time history of a multi frequency sinusoid of 2 Hz and 20 Hz and its integrated waveform. As can be observed, the low frequency component dominates the integrated waveform and the oscillatory characteristic of the original high frequency component is much smaller in the integrated waveform. This resembles with the reconstructed displacement time history of the chimney in Fig. 4.2.

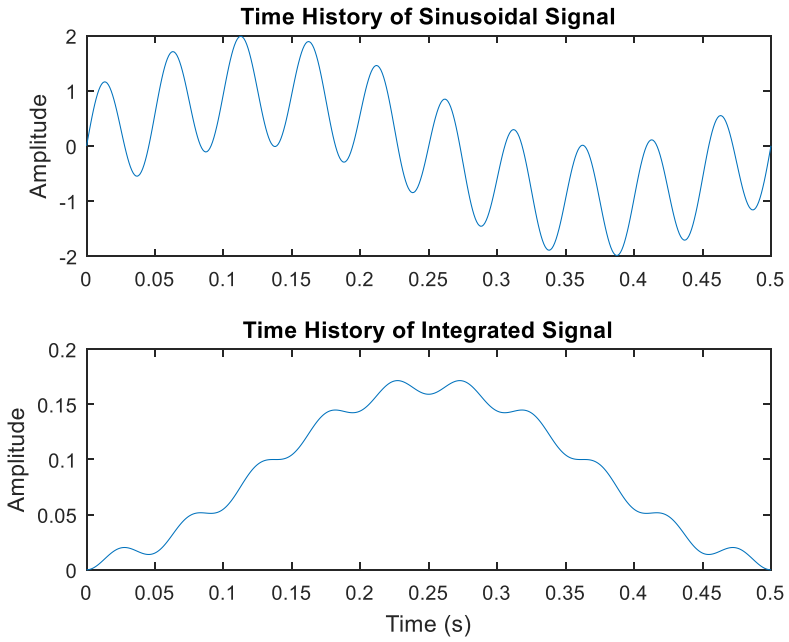

Fig. 4.5. Time history of multi frequency sinusoid and its integrated waveform.

4.3.2 Error due to constant (DC) offset

If a signal has constant component, the mean value (not the rms value) is not zero. A constant component can be caused by a constant bias in the analog voltage for whatever reason.

Let us consider an offset having an amplitude

(3.6)

the indefinite integral of y(t) is given as

(3.7)

which is an equation of ramp. It clearly shows that presence of a constant offset can completely change the shape of the integrated waveform.

One of the method to eliminate the error due to constant offset is to filter out the constant component or to extrapolate the measured acceleration to determine suitable initial velocity and displacement (Han 2010). The error due to domination of low frequency components is eliminated by applying a high pass filter before the integration of the waveform. A high pass filter is easy to apply with the frequency domain method, as discussed in next section.

4.4. Frequency domain method of displacement reconstruction

A Fourier series is a representation of a function in terms of a summation of an infinite number of harmonic components with different amplitudes and phases. The amplitude and phase of a sinusoid can be combined into a single complex number, called a Fourier coefficient. A Fourier series can be represented as

(3.8)

where, and are the Fourier coefficient and frequency respectively. In this method, we use the differentiation and integration properties of the Fourier transform to reconstruct the displacement from the measured acceleration. The Fourier transform of a continuous series is given by

(3.9)

where, ‘ ’ is circular frequency. So, the Fourier transform of first and second derivative of a series is given by

—— , (3.10)

—— (3.11)

(Oppenheim, Willsky et al. 1983). It is important to note that the above properties hold true for the discrete Fourier series as well. Since the acceleration $a(t)$ is the second derivative of $d(t)$, from the above equations 3.9 and 3.11, the discrete Fourier transform of the acceleration is

(3.12)

where, and are the discrete Fourier transforms of acceleration $a(t)$ and displacement $d(t)$ respectively. The time history of the displacement is obtained by taking the inverse discrete Fourier transform of which is represented as

— (3.13)

where, ——. This is the final equation for the determination of displacement time history if the time history of acceleration is known or measured. Figs. 4.6. and 4.7

show the time history of measured acceleration and reconstructed displacement of the hydraulic actuator and the chimney respectively using the frequency domain method.

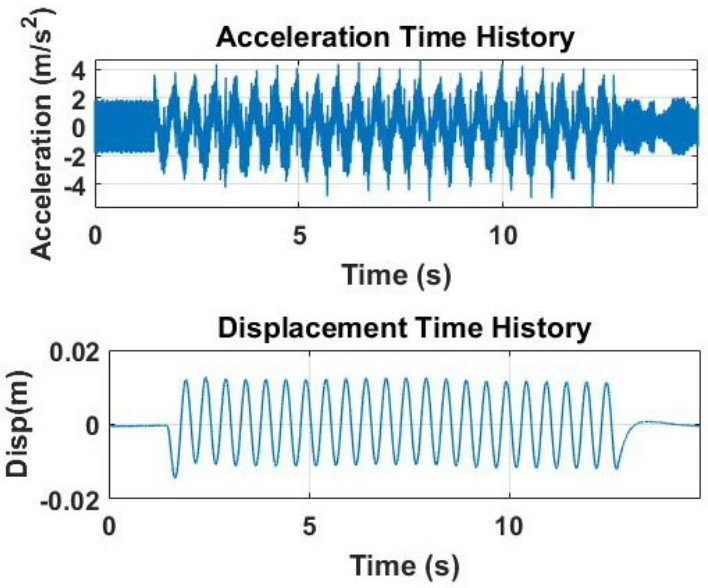

Fig. 4.6. Time history of reconstructed displacement from acceleration measured on the hydraulic actuator using frequency domain method.

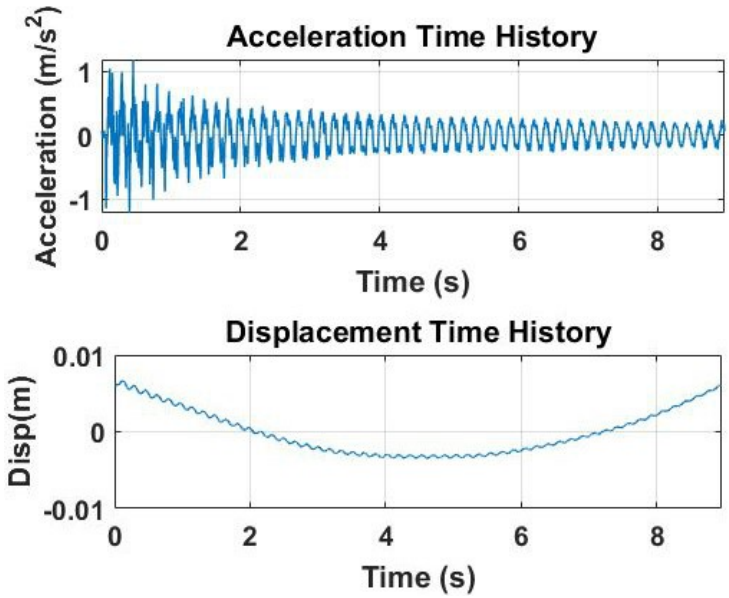

Fig. 4.7. Time history of reconstructed displacement from acceleration measured on the chimney actuator using frequency domain method.

It is now clear that frequency domain method works well for the acceleration time history which has a dominant single frequency as with the hydraulic actuator. On the other hand, the displacement time history of the chimney, as shown in Fig. 4.7, is of distorted shape and has a significant spurious low frequency component. So, this method must be improved to make it general, as discussed next.

4.5. Introduction of high pass filter

The Fourier transform of the single frequency signal is the delta function $\delta(f-f_0)$ where f_0 is the frequency of the signal. So, all the Fourier coefficients should be zero except at frequency value f_0. But, due to leakage, each Fourier coefficient actually has non-zero value. Also, noise pollutes the signal. Thus, in spite of having a single frequency of vibration spurious low frequency and high frequency components appears in the transformed signal as shown in Fig. 4.8.

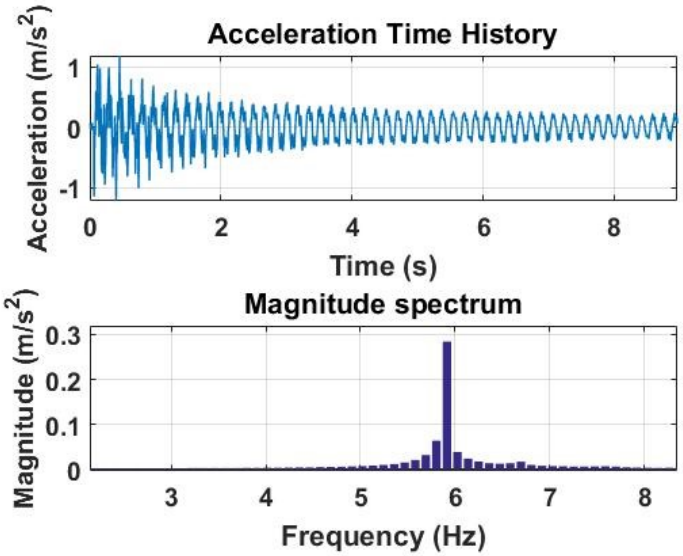

Fig. 4.8. Fourier transform of acceleration time history of the chimney.

Since, before inverse transform of to obtain the displacement time history, Fourier transform of acceleration time history is divided by negative square of the angular frequency - ^{2}. Thus, lower frequency components dominate the displacement time history. On the other hand, error due to high frequency components disappear because of very small magnitude obtained by dividing by the large number, that is the square of high frequency components.

To convert a measured acceleration signal to a displacement signal with minumum errors using the frequency domain method, we need to remove the error caused by erroneous low frequency components caused by various sources. We use the high pass filter to eliminate this error. In nutshell, we select a value of cut-off frequcency depending upon the predominant frequency of the signal and all the frequencies below the cut-off are removed before dividing by the negative square of the angular frequency. This gives much improved results, as shown in Fig. 4.9.

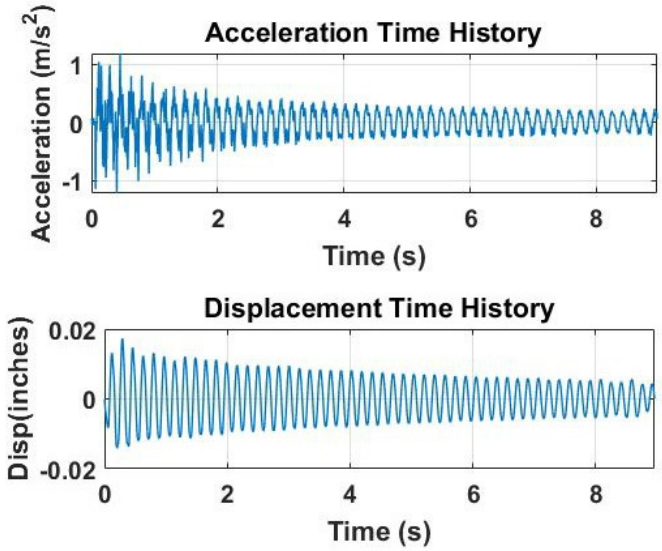

Fig. 4.9. Reconstructed displacement of chimney using high pass filter on frequency domain method.

For this case the cut-off frequency of 4 Hz is selected as the predominant frequency of vibration of the chimney is known by other consideration to be 5.9 Hz. The cut-off frequency can be selected by judgement or by a trial and error process until a plausible displacement time history is obtained.

4.6. Summary

It is quite easy using MATLAB, to apply the mathematical integration techniques for calculating displacement time history from measured acceleration time history. However, when data contains even a small amount of spurious low frequency or constant offset components then this method fails to adequately predict the displacement time history.

The Fourier transform can be used to reconstruct displacement. Errors in this method can be diminished by using the high pass filter. The success of this method depends on the reasonable selection of the cut-off frequency. The cut-off frequency can be selected accurately only if we know what frequencies we are interested in.

Thus, reconstruction of the displacement time history from measured acceleration data remains more art than science.

Chapter 5 Free Vibration Study of the Doghouse

This chapter's objectives are to:

- provide the reader with some background on free vibration of structures;
- introduce finite element and laboratory models of the doghouse;
- discuss the finite element and the experimental analysis of the vibration of the doghouse.

5.1. Introduction

It often happens that we need to measure the dynamical properties of an engineering system. For example, we might want to measure the natural frequencies and damping coefficients of a structure after it has been built to make sure that the design predictions were correct. Also, the natural frequencies and mode shapes of structures might contain information about the location and dimension of damage which can be used for structural health monitoring purposes.

Let us consider a spring-mass-dashpot system, as shown in Fig. 5.1.

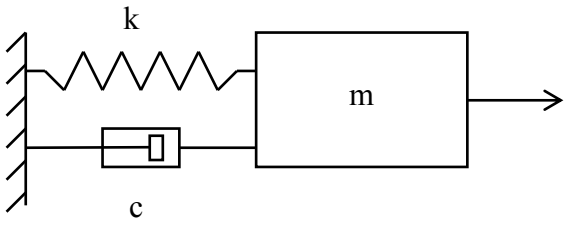

Fig. 5.1. Damped spring-mass-system.

The unforced equation of motion for the damped spring-mass-system is given by

, (4.1)

where is the mass of a system, is the damping coefficient, is the stiffness of the spring, and is the displacement response.

Although the single-degree-of-freedom (SDOF) model might adequately describe the dynamical behavior of some systems, in most real structures it is necessary to employ more complex multiple-degree-of-freedom (MDOF) models. The equation of motion of a linear MDOF model of a structure is

, (4.2)

where is the mass matrix, is the damping matrix, is the stiffness matrix, is the acceleration vector, is the velocity vector, and is the displacement vector. These coefficient matrices are all N x N matrices where N is the number of degrees of freedom. The acceleration vector , the velocity vector , the displacement vector , and the load vector are all N x 1 vectors (Craig and Kurdila 2006).

The unforced equation of motion for an undamped MDOF system, written in matrix form is

, (4.3)

where is displacement vector, assumed to be harmonic as

(4.4)

where is the amplitude vector, is the angular frequency, is the phase angle and is time. Substituting Equation 4.4 into Eq. 4.3 gives

(4.5)

(Craig and Kurdila 2006). This is called the frequency equation or the characteristic equation and is an eigenvalue problem. Each eigenvalue corresponds to a natural frequency of vibration, and for each eigenvalue there will be an eigenvector which corresponds to a natural mode of vibration.

5.2. Description of the laboratory structure

The main purpose of the research is to conclude whether we can identify the types and locations of machines concealed within buildings using vibration information gleaned from the building envelopes. Structural vibrations can be sensitive to minor details. For example, a steel building experiencing vibration vibrates differently when the connections are tight than when some connections are loose. Thus, detailed study of the structure may be required before using the vibration signatures obtained from it to predict the types and locations of concealed machinery. However, it is difficult to accurately model a complex building like the Ford Utility Building, which will be described later. Thus, a simplified model is built in the laboratory which represents a simplified industrial building hereafter called the "doghouse".

The doghouse is a one-story 48''x 30''x 30" cuboidal building with a 12" diameter chimney of sixty-inch height. It is constructed from sheet metal plates connected with screws to a 1.5"x 1.5" pine framework. Figs 5.2, 5.3, and 5.4 shows the construction drawings of the doghouse. Figs 5.5 and 5.6 shows the photographs of constructed doghouse. Tolerance of ± 1/16" was adopted.

a) Short Side Wall

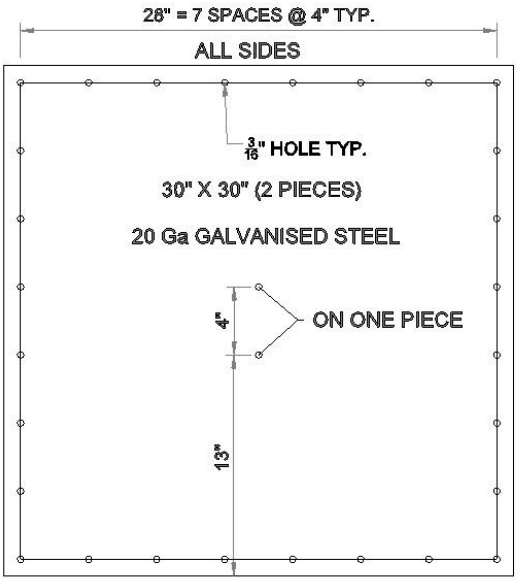

b) 6” Bent Plate Connector A

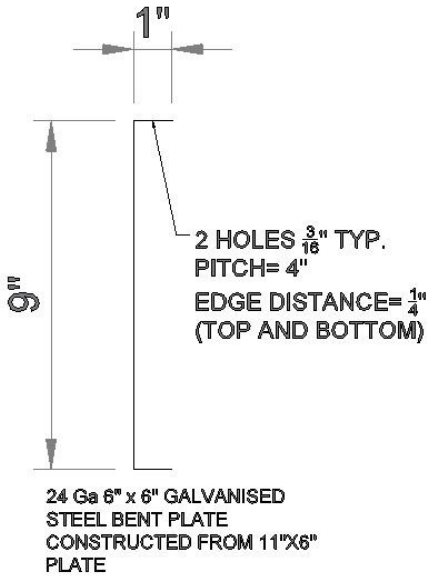

c) 9” Bent Plate Connector B

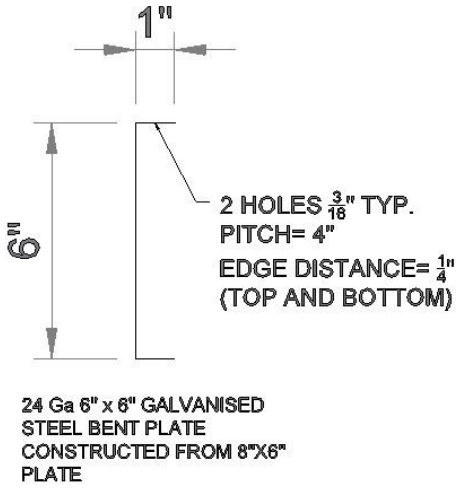

d) 2D View of Chimney

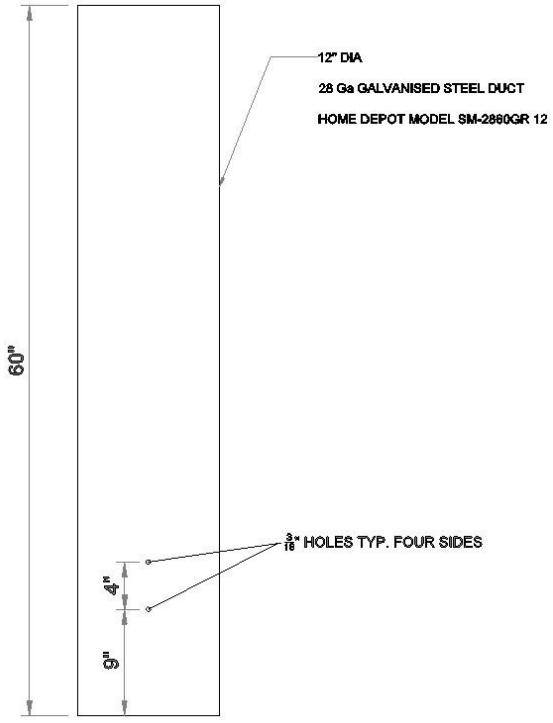

Fig. 5.2. Construction drawings of the doghouse.

e) Long Side Wall

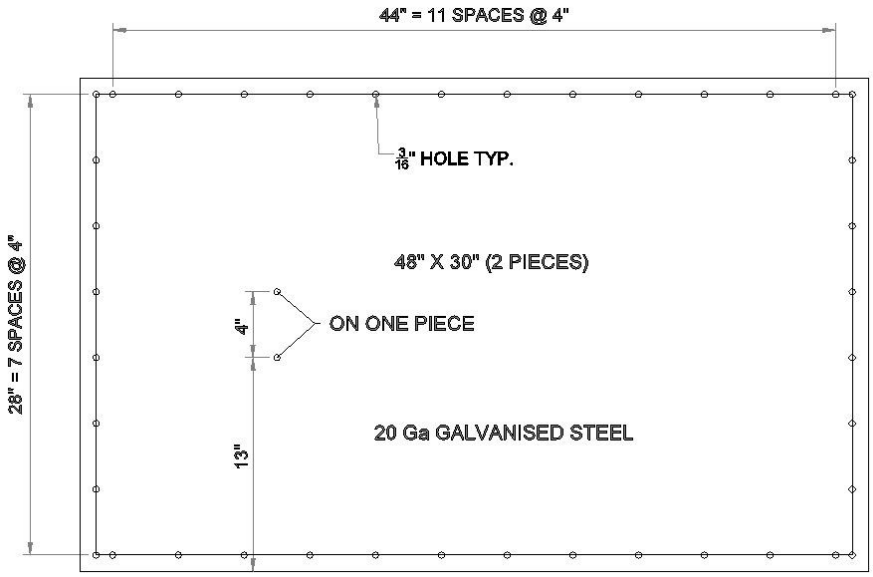

f) Roof

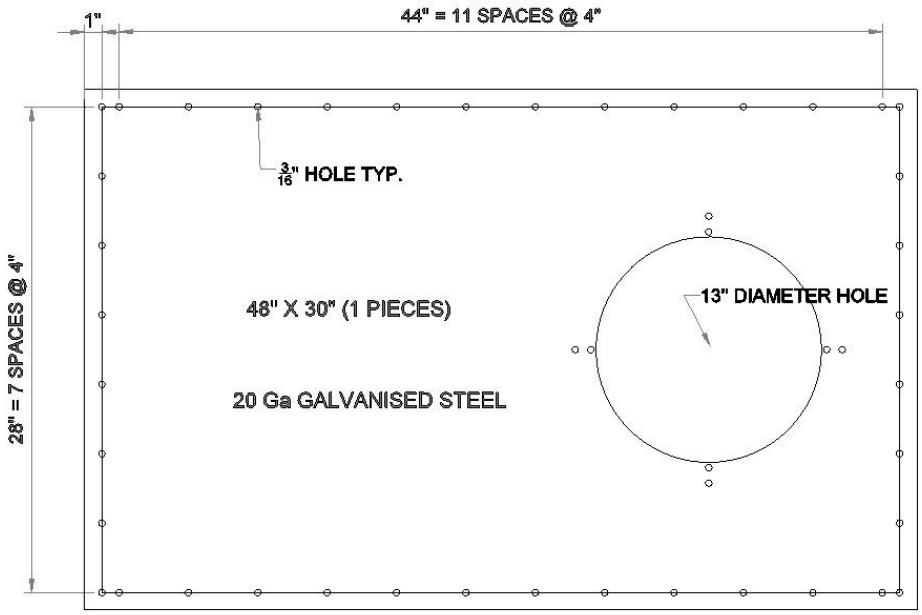

Fig. 5.3. Construction drawings of the doghouse.

g) Plan view of the doghouse

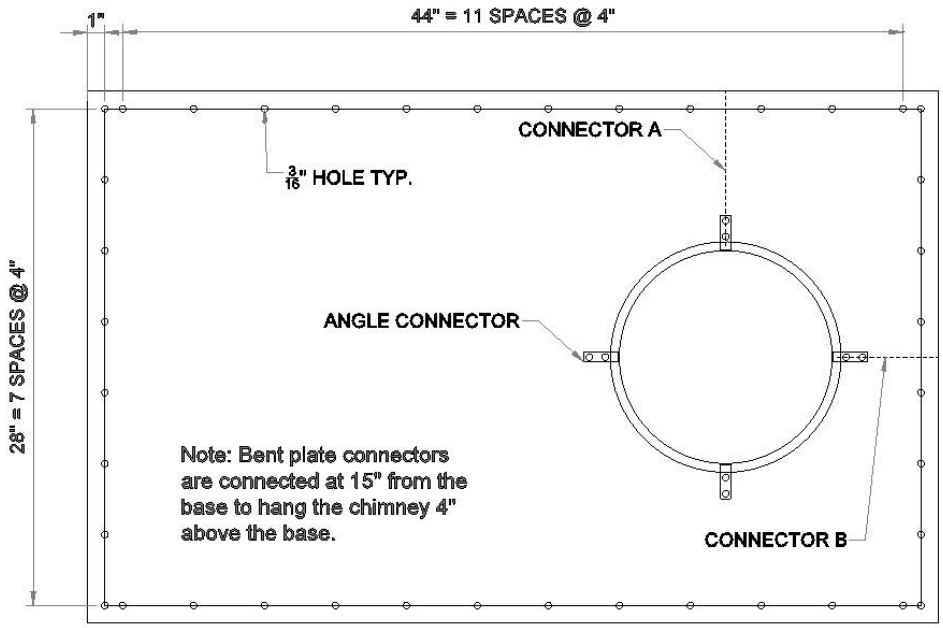

h) Angle Connector

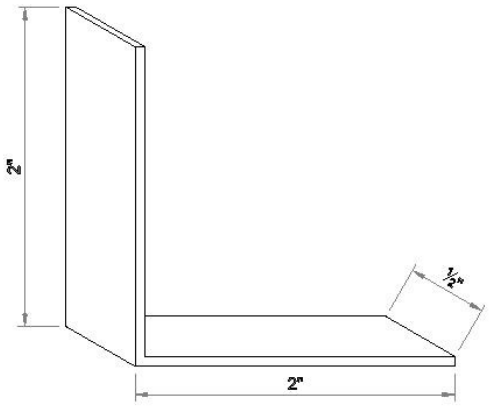

ANGLE CONNECTOR (4 PCS)

Note:
4 Pieces of 1.5"x1.5" pinewood of 48" long
8 Pieces of 1.5"x1.5" pinewood of 27" long
1 Piece of 60"x38"x0.5" Oriented Strand Board (OSB)

Fig. 5.4 Construction drawings of the doghouse.

Fig. 5.5. Doghouse.

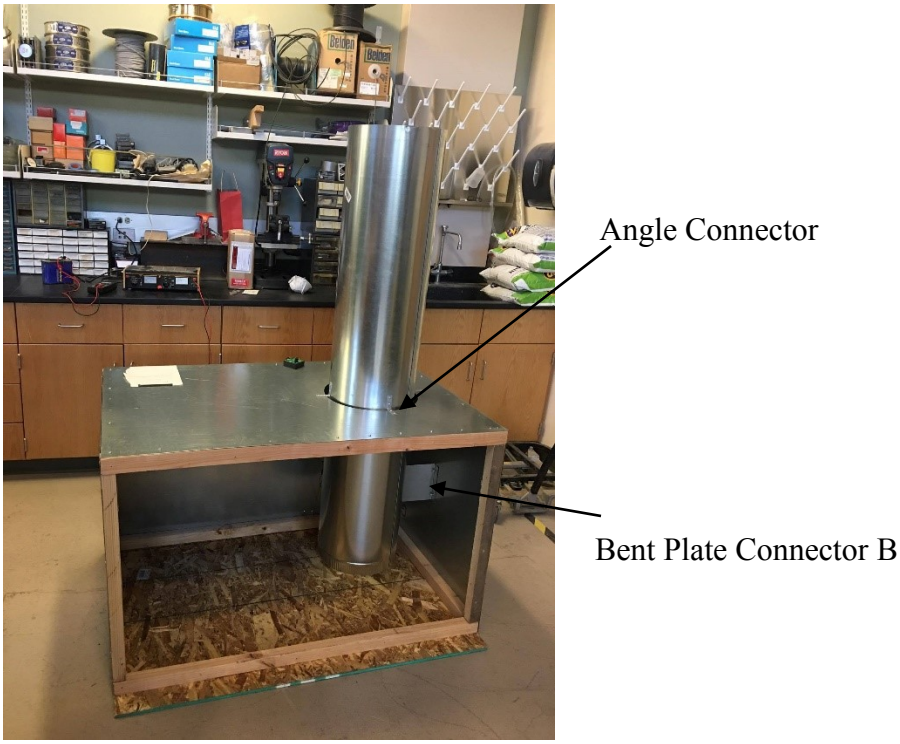

Fig. 5.6. Connection of chimney with roof and walls. Front wall removed.

The chimney is connected to the roof with the four angle connectors and the chimney is also connected with the two adjacent walls with bent plate connectors to support the chimney four-inches above the base, as shown in Fig. 5.6. The doghouse is finally connected to a half-inch thick wood oriented strand board (OSB) base.

5.3. Finite element analysis

We next use a finite element program to perform free vibration analysis of the doghouse and compare the results obtained from the finite element analysis with the experimental results, and hence to see how accurately the finite element software can model a real structure.

The finite element model of the doghouse is developed using SAP2000. The model includes shell elements to represent walls, roof, chimney, and plate connectors as well as frame elements to represent the wooden frame, and angle connections, as shown in Fig. 5.7.

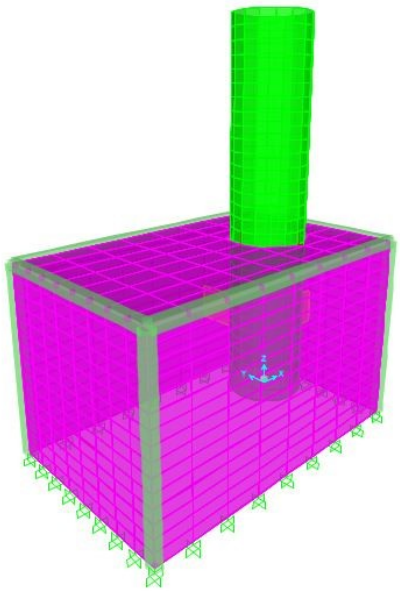

Fig. 5.7 Finite element model of the doghouse using SAP2000.

The doghouse geometry is modeled exactly is shown in Fig. 5.7, but have some simplifications were used in modeling the connections. The doghouse has an OSB base but is modeled as having a clamped support at its base. Instead of using bent plate connectors used in the doghouse, straight plate connectors are used in the model. The sheet metal plates in the doghouse are connected with screws to a pine framework on every 4-inch gap but is modeled by connecting the wooden frames and steel plates at their nodes as shown in Fig. 5.7. Similarly, instead of using angle connectors to connect the chimney and the roof, rectangular frame elements of same cross section area as an angle connector are used to connect the roof and the chimney making L shaped connections.

Modal analysis is performed to determine the mode shapes and natural frequencies of vibration of the doghouse. The fundamental frequency of vibration of the doghouse is found to be 5.40 Hz. Figs. 5.8 and 5.9 show the first mode and the second mode of vibration of the doghouse. The natural frequency of second mode of vibration is found to be 8.474 Hz.

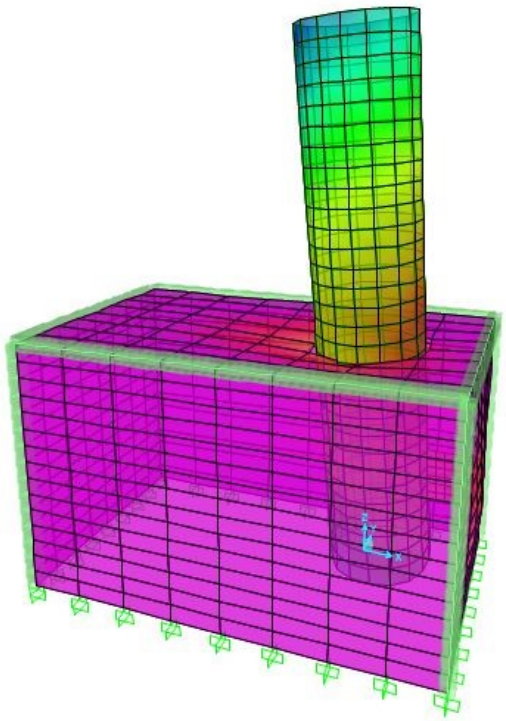

Fig. 5.8. First mode of vibration of the doghouse using SAP2000.

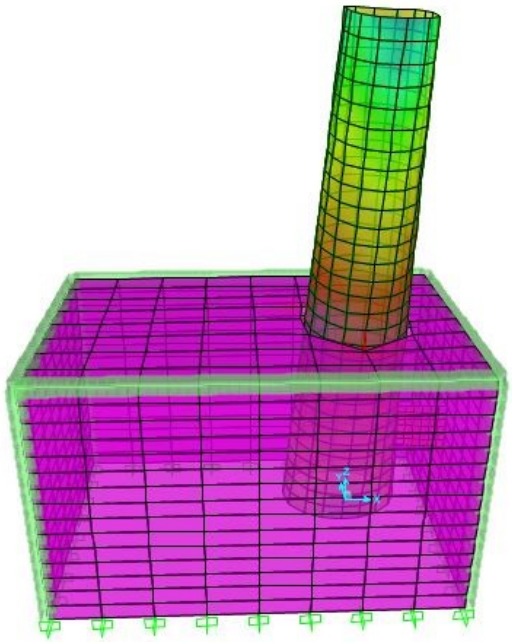

Fig. 5.9. Second mode of vibration of the doghouse using SAP 2000.

5.4. Experimental analysis

Experiments were performed in the lab to determine the frequencies of vibration of the doghouse. Fig. 5.10 shows the experimental setup to determine the free vibration of the chimney.

Fig. 5.10. Experimental setup to measure free vibration of the chimney.

As shown in Fig. 5.10, an accelerometer is attached near the top of the chimney using double-sided tape to record the acceleration during the free vibration of the chimney.

The top of chimney was perturbed about ½ inch by hand and suddenly released, causing free vibration. The acceleration is measured using an accelerometer and LabVIEW as discussed in Chapter 3. Data is processed with Discrete Fourier Transform

(DFT) in MATLAB, producing the frequency and acceleration magnitude of the vibration, as shown in Fig. 5.11.

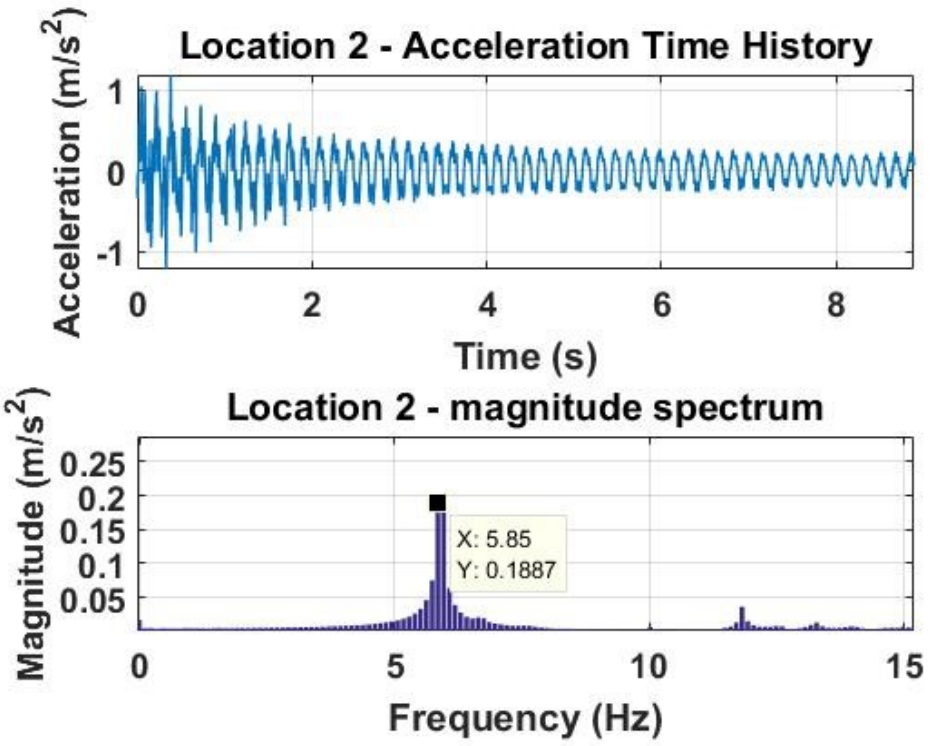

Fig. 5.11. Damped free vibration time history, and magnitude spectrum of chimney of the doghouse, measured by the accelerometer.

In Fig. 5.11. we observe multiple peaks in the magnitude spectrum. It might be due to noise from other vibrating source in the laboratory. The fundamental frequency of vibration of chimney is apparently 5.85 Hz.

Fig. 5.12. shows the experimental setup to record the free vibration of roof of the doghouse. In this case the accelerometer is attached to the roof and free vibration is activated by perturbing chimney by hand and releasing it suddenly as before. Acceleration is measured again using the accelerometer and LABVIEW.

Fig. 5.12. Experimental setup to measure the free vibration of the roof.

The time history data obtained from LabVIEW is again processed with Discrete Fourier Transform (DFT) in MATLAB to obtain the frequency and acceleration magnitude of vibration. Fig. 5.13. represents the time history of damped free vibration of roof of the doghouse with some noise but less than in the case of the chimney. The roof vibrates with the fundamental frequency of 5.881 Hz.

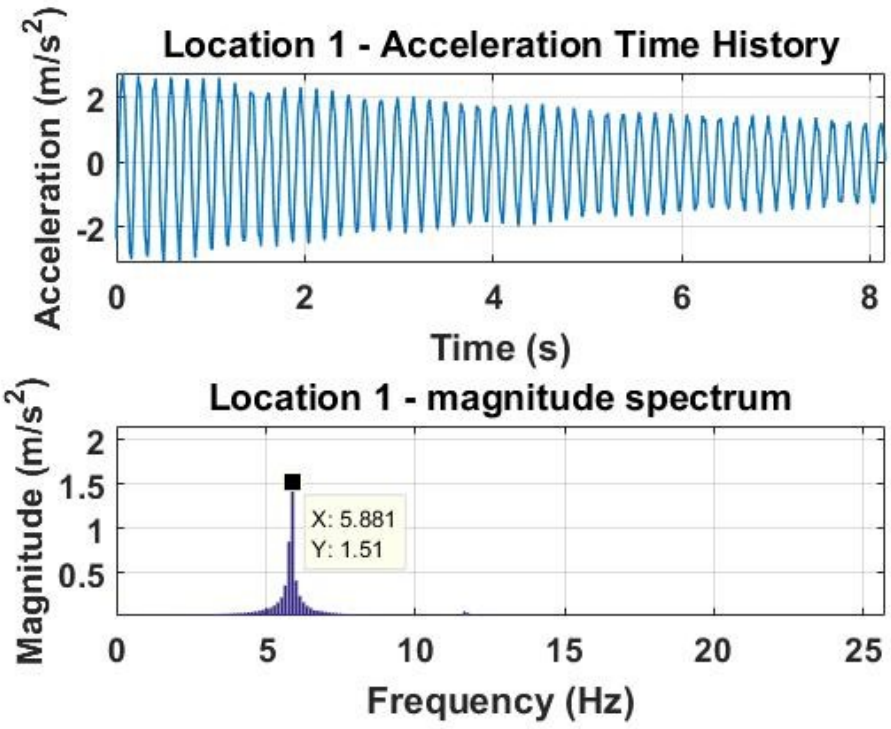

Fig. 5.13. Damped free vibration time history and magnitude spectrum of roof of the doghouse, measured by accelerometer.

As can be observed, the fundamental frequency of both chimney and roof determined by the experimental analysis matches closely. Hence, we conclude that the fundamental frequency of the doghouse is approximately 5.8 Hz ± 0.1 Hz.

5.5. Summary

In the development of finite element model of structures, it is necessary to make some simplifying assumptions which may lead to discrepancies between the finite element results and the experimental results. Table. 5.1 shows the lack of agreement between numerical result and experiment result.

Table. 5.1. Fundamental frequency of the doghouse predicted by SAP2000 and experiment.

Method	Fundamental Frequency (Hz)
Finite element (SAP2000) prediction	5.40
Experimental analysis using DFT	5.85 (center of roof) and 5.881 (top of chimney)

The numerically predicted fundamental frequency is 8% lower than the experimental result. This discrepancy might be due to the simplifications used in the finite element model and also might due to the nonlinear behavior of the doghouse. Although the discrepancy is not that high, the fundamental mode shape of vibration predicted by SAP2000 does not match with the experimental results. This led us to study more closely the structure and its behavior, which will be discussed in next chapter.

Chapter 6 Refined Vibrational Models of the Doghouse

This chapter's objectives are to:

- provide the reader with some background on nonlinear vibration of plates;
- study the effect of connections on vibration;
- study the effect of stress stiffening on vibration;
- compare the numerical and the experimental results of vibration of the doghouse.

6.1. Introduction

We have introduced the free vibration analysis of the doghouse in Chapter 5. We found there is a discrepancy between the linear finite element results and the experimental results. We suspect this discrepancy is due to two major causes. First, due to simplifications made while modeling the connections in SAP2000. Second, due to the nonlinear vibrational behavior of the doghouse. This prompts us to study the behavior of the doghouse more closely.

In this chapter, first we simplify the geometry of the doghouse. This is done to clarify the numerical modeling and the experiments. The chimney is removed from the doghouse. Also, the roof with the hole is replaced by an identical plate without a hole, as shown in Fig. 6.1.

We next conduct nonlinear finite element analyses and experimental tests to investigate the frequency of vibration of the doghouse. With the nonlinear finite element analyses, we include the nonlinearity due to deformation of the doghouse under the gravity. We find the resulting nonlinear model compares better than the linear finite element method with the experimental results.

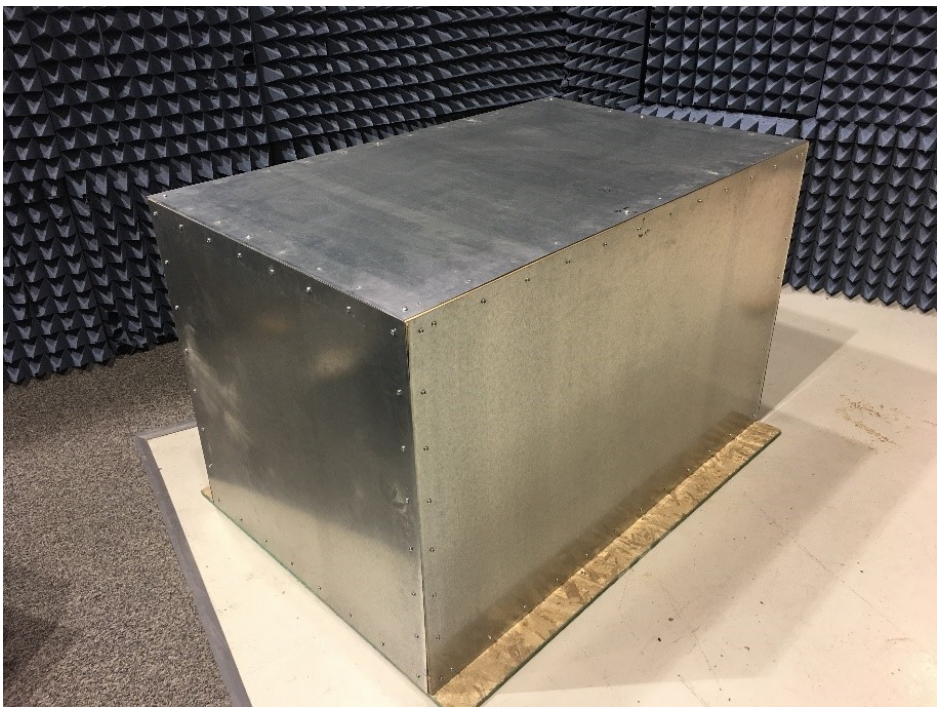

Fig. 6.1. Doghouse after removal of the chimney and hole in the roof.

Additionally, we perform experiments to study the effect of connections on the frequency of vibration of the doghouse and compare with the finite element results. We find that the frequency of vibration varies with respect to the number of screws connecting the steel plates to the wooden frame members.

6.2. Nonlinearity

"Structural nonlinearity" means that the displacement response is not linearly related to the applied force. There are several sources of nonlinearity.

One source is material nonlinearity. Material nonlinearity occurs when the stress no longer proportional to the strain. No material is perfectly linear elastic. The assumption of linear elastic material behavior is used to simplify the calculations, and this

approximation is satisfactory to most situations. Materials like rubber have nonlinear elastic properties. Material nonlinearity is not considered in this Chapter.

Another cause of structural nonlinearity is geometric nonlinearity. Geometric nonlinearity is important for plates, when transverse deflection is more than the plate thickness. In such cases, the assumption of linear behavior is far from the truth. Such problems are called “large deflection problems”. With a thin plate, when the transverse displacement exceeds the thickness of the plate, mid-plane stretching, called the “membrane effect” occurs. The out-of-plane stiffness of a plate can be significantly affected by membrane stresses. This coupling between membrane stress and bending stress is known as “stress stiffening”. The Von Karman, or large deformation theory, of plates accounts for such geometric nonlinearity in its derivation (Levy 1942).

Duffing’s model is an example of nonlinearity involving a nonlinear spring in a mass-spring-damper system. The equation for free vibration motion is

(5.1)

where is the mass, is the damping coefficient, is the stiffness, is the cubic stiffness coefficient, is the acceleration, is the velocity and is the displacement of a mass-spring-damper system.

This list of nonlinearities is far from complete. Nonlinearity exists due to many sources. In fact, the assumption of linearity is just an approximation to make the model simpler. This simplification allows the advantages of superposition and uniqueness. However, it is important to understand when the use of a nonlinear theory is necessary (Sathyamoorthy 1987).

6.3. Nonlinearity based on the deformations of an elastic plate

A plate is a planar elastic continuum that resists bending moments. In deriving the equation of motion of a plate some simplifying assumptions are made to allow linear behavior. First, we assume is that there is a plane which is unstressed called neutral plane which exists if we do not have in-plane forces. On the neutral plane, there is no in-plane strain due to the small transverse deformation. The second assumption we make is that there is no shear deformation. This is also known as the Kirchhoff hypothesis. The third assumption we make is that the deformation gradients are small. The equation of motion for a free vibration of a Kirchhoff plate is

— (5.2)

where is the flexural rigidity of the plate, is the out-of-plane displacement, is the density and is time (Leissa 1969). The solution obtained from Equation 5.2 may yield inaccurate results if deflections are greater than one tenth of the plate thickness. When plate deflections are larger than one-tenth of the plate thickness, a more rigorous theory that takes account of membrane strain should be used.

When a thin elastic plate undergoes large deflection (approximately), where is the transverse deflection and is the thickness of a plate, the middle surface of the plate stretches. Thus, the strain versus displacement relations become nonlinear. The two in-plane displacement components and , and the transverse displacement are interrelated. The strain displacement relations for large deflection of a plate are

— - — (5.3)

— - — (5.4)

— — —— (5.5)

where and are rectangular coordinates, is the strain in x direction, is the strain in y direction, is the shearing strain in the middle plane of a plate, and are the in-plane displacements, and is the transverse displacement. The nonlinear terms above couple the transverse displacement with the in-plane displacement (Timoshenko and Woinowsky-Krieger 1959). The equation of free vibration of a geometric nonlinear plate can be derived using above strain equations. However, this is beyond the scope of this thesis. Instead we use nonlinear finite element analysis to study the nonlinear vibration of a plates.

6.4. Laboratory tests of the doghouse

Experiments are performed in the laboratory to determine the fundamental natural frequency of the doghouse. In this section, we first present the measurement of the fundamental frequency of the roof, and then that of the long sidewall of the doghouse. Because the roof sags due to its weight, we expect the roof to be stiffer than the sidewalls, and thus to vibrate at higher frequency than the sidewalls. Also, we study the fundamental frequency of the roof and the wall as we vary the number of connecting screws. It is important to note that throughout the experiment all the screws are firmly tightened by a handheld screwdriver.

6.4.1 Free vibration of the roof

In the following subsections, we present the measurement of vibration of the roof with three different categories of connection types. First, only the holes at the corners and the center of each edge of the roof have screws. This is termed as “connection type A”. Second, only the holes at the corners and at every other hole of each edge of the roof have screws. This is termed as “connection type B”. Finally, all the holes on each edge of the roof have screws. This is termed as “connection type C”. For all three categories, we only vary the number of connecting screws on the roof. The remaining four walls are connected with the screws in each hole.

Fig. 6.2 shows the experimental setup to measure free vibration at the center of the roof.

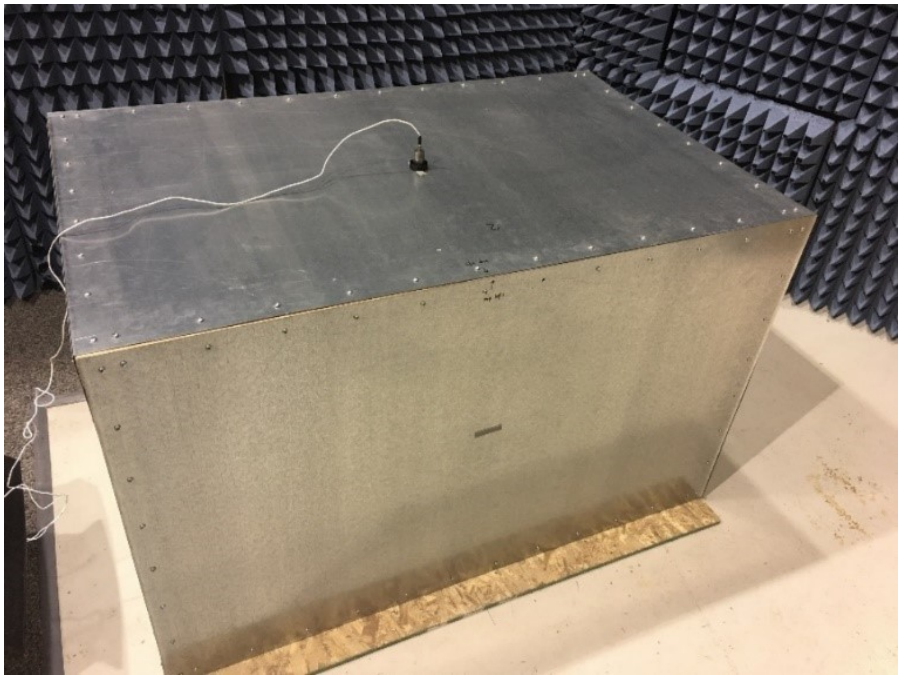

Fig. 6.2. Experimental setup to measure free vibration of the roof with an accelerometer.

The center of the roof is perturbed about ½ inch in the vertical direction by hand and suddenly released to cause free vibration. Vibration of the roof for all three connection types are recorded by the accelerometer attached at the center of the roof, as shown in Fig. 6.2. The Time history of acceleration is processed with Discrete Fourier Transform (DFT) in MATLAB, producing the fundamental frequency and acceleration magnitude of vibration. The fundamental frequency of vibration of the roof for connection type A, B, and C are found to be 12.6 Hz, 13.7 Hz, and 15.06 Hz, as shown in Figs 6.3, 6.4, and 6.5 respectively. These experiments show that the fundamental frequency of the roof increases as we increase the number of screws connecting the roof to the wooden framing members.

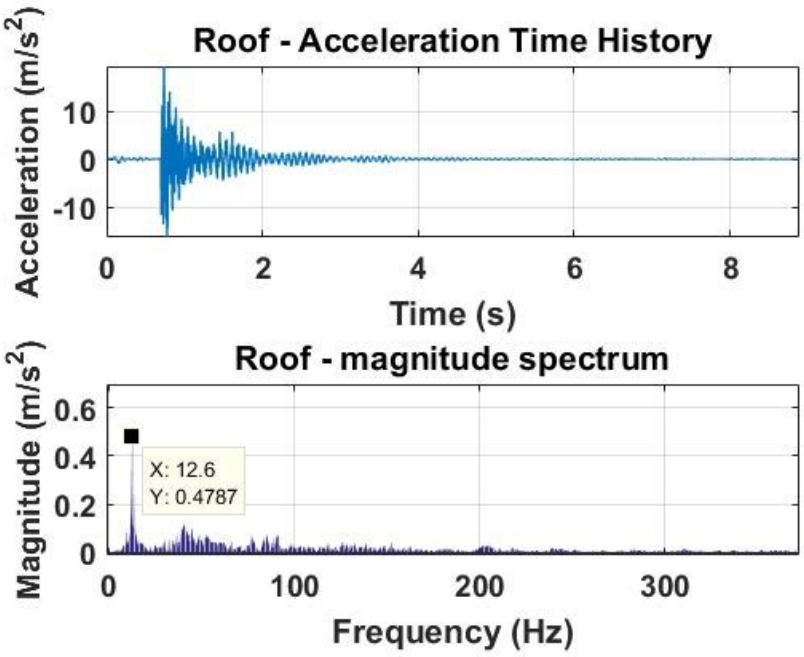

Fig. 6.3. Time history and magnitude spectrum of vibration of the roof for connection type A.

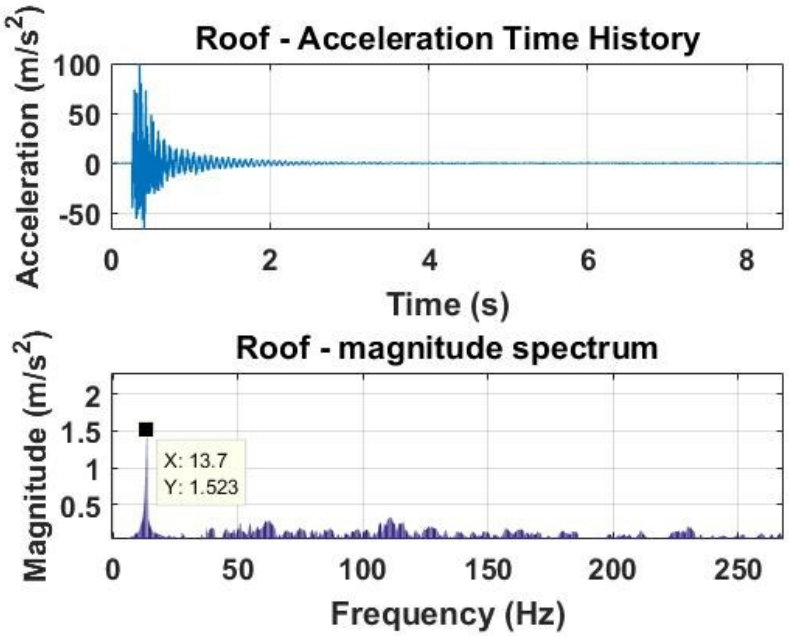

Fig. 6.4. Time history and magnitude spectrum of vibration of the roof for connection type B.

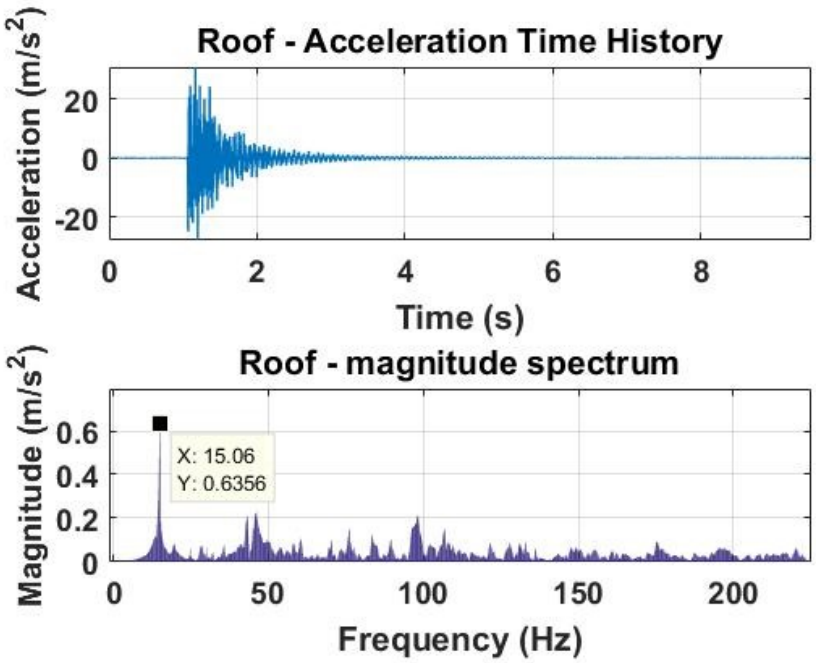

Fig. 6.5. Time history and magnitude spectrum of vibration of the roof for connection type C.

6.4.2 Free vibration of the long sidewall

In the following subsections, we present the measurement of vibration of one of the longer sidewalls in three different categories of connection types A, B and C, as done in the roof. Similarly, for all three connection types, the remaining three walls and the roof of the doghouse are fully connected with screws in each hole.

As with the roof, the center of the long sidewall is perturbed about ½ inch perpendicular to the plane of the wall by hand and suddenly released to cause free vibration. Fig. 6.6 shows the experimental setup to measure free vibration at the center of one of the long sidewalls.

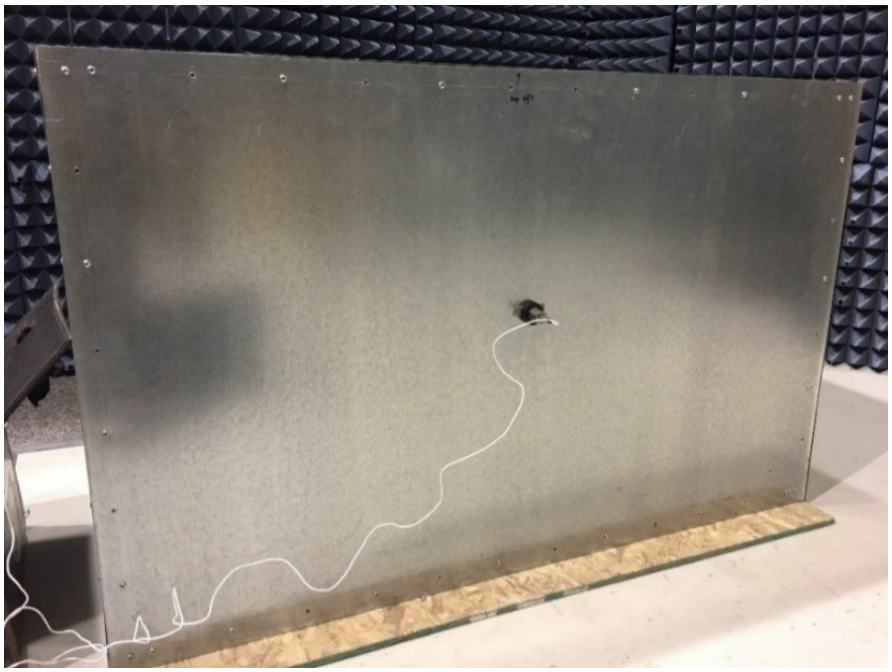

Fig. 6.6. Experimental setup to measure damped free vibration at the center of the long sidewall using an accelerometer.

Vibration of the long sidewall for all three connection types are recorded and processed using the DFT to determine the fundamental frequency of vibration. The fundamental frequencies of vibration of the long sidewall for connection types A, B, and

C are found to be 9.483 Hz, 11.07 Hz, and 11.78 Hz, as shown in Figs 6.7, 6.8, and 6.9 respectively. Like with the roof, these experiments also show that the fundamental frequency of the long sidewall increases as we increase the number of screws connecting the long sidewall to the wooden frame.

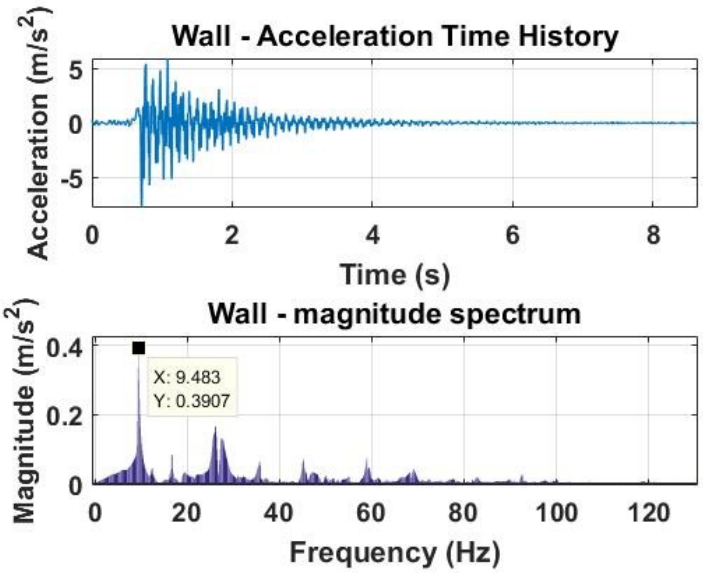

Fig. 6.7. Time history and magnitude spectrum of vibration of the long sidewall for connection type A.

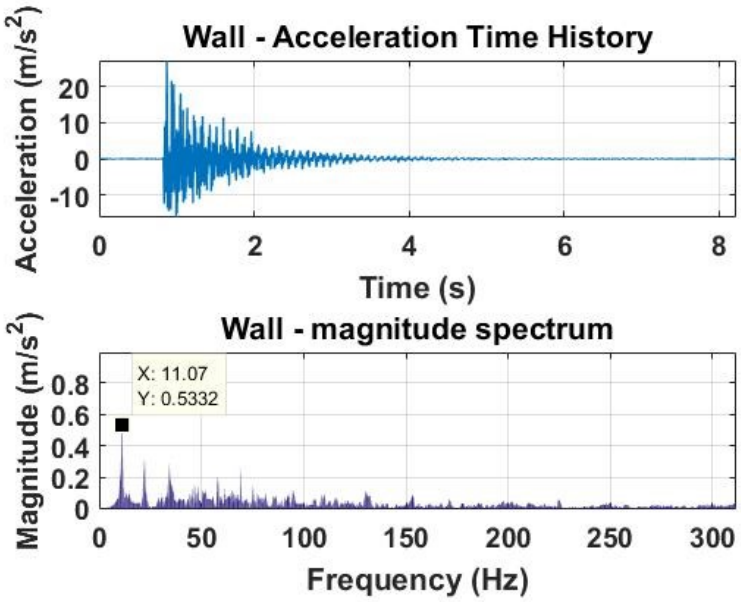

Fig. 6.8. Time history and magnitude spectrum of vibration of the long sidewall for connection type B.

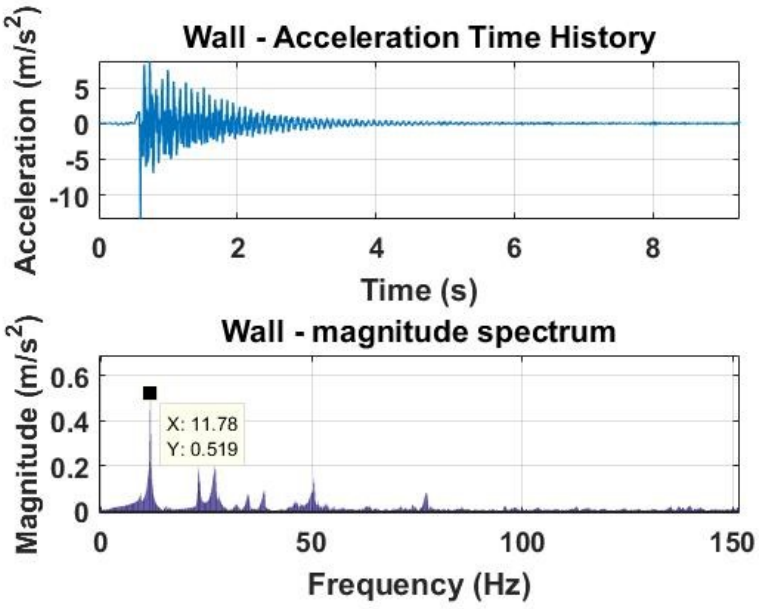

Fig. 6.9. Time history and magnitude spectrum of vibration of the long sidewall for connection type C.

6.5. Finite element analysis of the doghouse

To gain perspective on the experimental and theoretical discussions presented above, finite element analyses are conducted. To observe the difference in results, both linear and nonlinear finite element models are presented in the following subsections. We find that the linear model fails to explain the experimental results. Thus, the nonlinear finite element model is studied in greater depth than the linear model.

6.5.1 Linear finite element model

The finite element model of the doghouse with connection type C is developed using SAP2000, as shown in Fig. 6.10. While modeling, steel frame elements of 1/8-inch diameter and Modulus of Elasticity 29000 Psi are used to model the screws connecting the steel plates to the wooden frame members. All the other parts are modeled as in

Chapter 5. Modal analysis is performed to determine the mode shapes and natural frequencies of vibration of the doghouse. The fundamental frequency of vibration from linear finite element approach is found to be 10.36 Hz, as shown in Fig. 6.10.

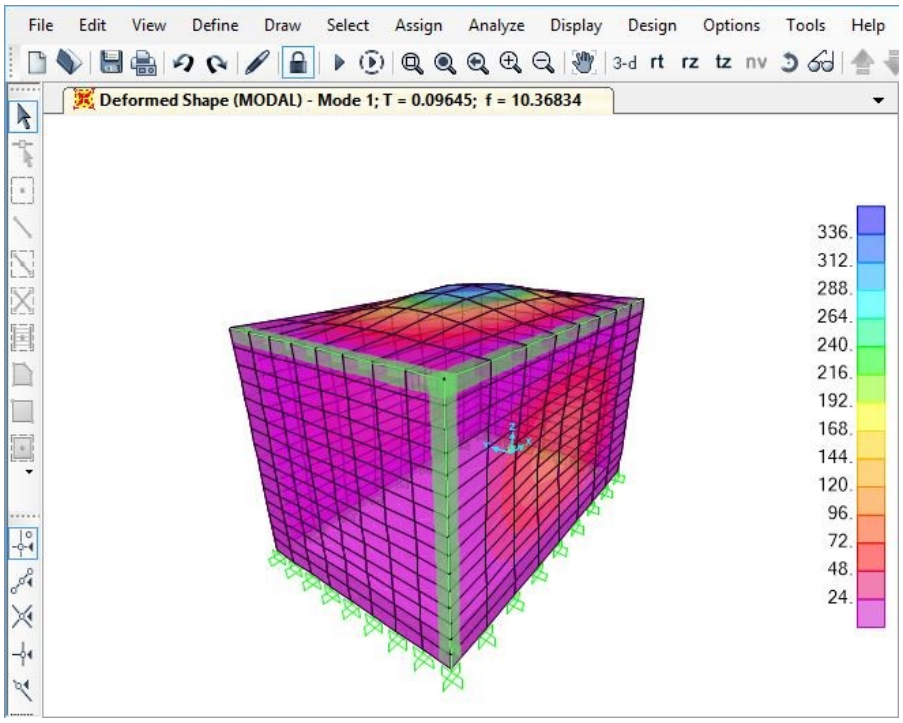

Fig. 6.10. Fundamental mode of vibration (10.36Hz) of the doghouse with connection type C using SAP2000.

As can be observed, linear finite element approach predicts the same fundamental frequency for the long sidewall and the roof. However, experimental results show the roof has a higher frequency than the long sidewall. We next use a nonlinear finite element model to predict the fundamental frequency of the doghouse.

6.5.2 Nonlinear finite element model

In this subsection, first, we perform linear and nonlinear static analysis to find the reason behind the lack of agreement between linear finite element model and

experimental results. Then, we perform a modal analysis to determine the fundamental frequency of the doghouse using the nonlinear finite element approach.

The linear and nonlinear static analysis is performed under the gravity load using SAP2000. Fig. 6.11 shows the vertical deflection of the roof during linear and nonlinear static analysis under the gravity load for connection type C.

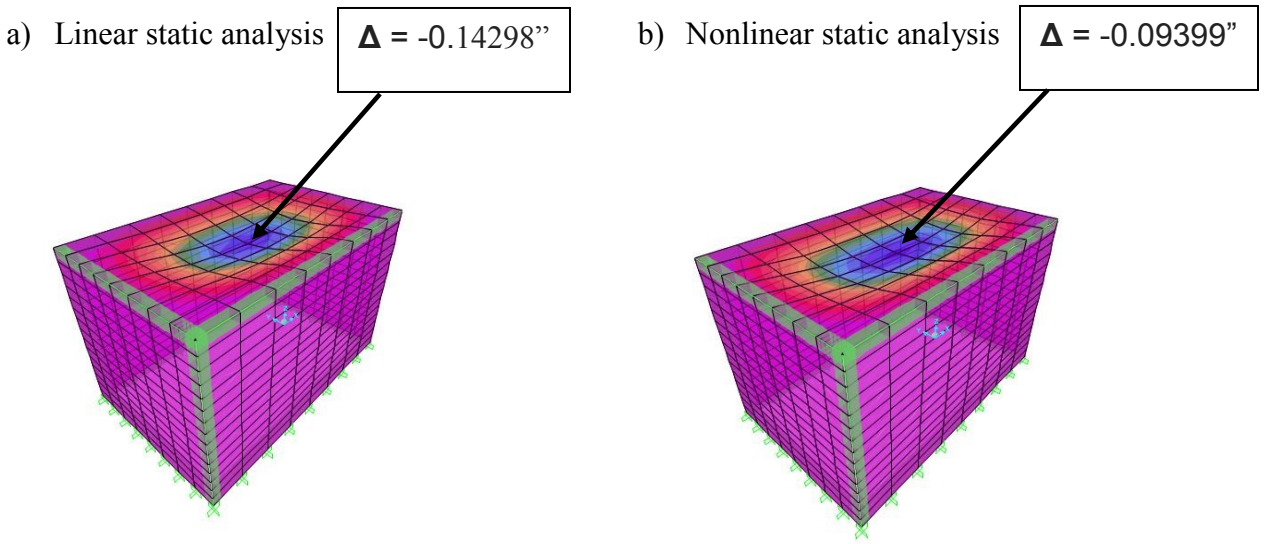

Fig. 6.11. a) Linear static analysis of the doghouse under the gravity load, and b) Nonlinear static analysis of the doghouse under the gravity load for connection type C.

The vertical deflection of the roof obtained from the linear static analysis is 0.14298” and the vertical deflection of the roof obtained from the nonlinear static analysis is 0.09399”. The deflection of the plate from the linear static analysis is found to be about 4 times greater than the thickness of the plate (0.0396”), which means it is a large deflection problem. Thus, the linear finite element model poorly represents the actual behavior.

Additionally, we observe the deflection obtained from the nonlinear static analysis is 35% less than the linear static analysis. This means the roof is stiffer than that predicted by the linear approach. This increase in stiffness of the roof is due to the stress stiffening effect.

We next perform modal analysis using the nonlinear finite element model. To account for the stress stiffening effect due to gravity, the stiffness obtained at the end of nonlinear static analysis is used as the stiffness for the modal analysis. Fig. 6.12 shows the first mode of vibration of the long sidewall and the roof. The fundamental frequency of the long sidewall is found to be 10.06 Hz and the fundamental frequency of the roof is found to be 15.45 Hz for connection type C.

a) Fundamental mode shape of the wall

Frequency = 10.06358 Hz

b) Fundamental mode shape of the roof

Frequency = 15.45685 Hz

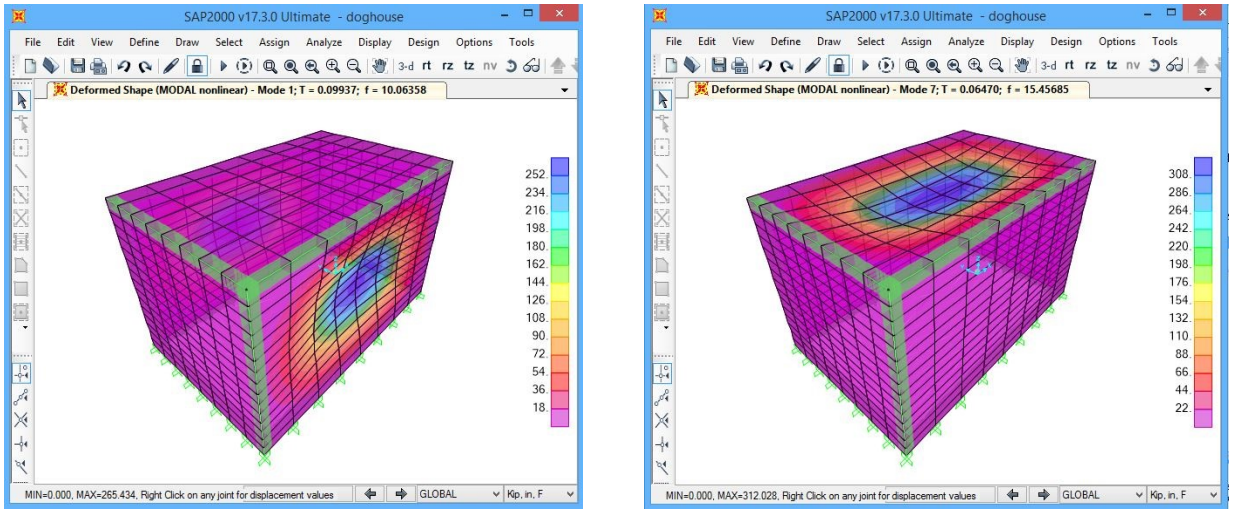

Fig. 6.12. a) Fundamental mode shape and frequency of the long sidewall and b) Fundamental mode shape and frequency of the roof for connection type C, using stress stiffened modes.

Thus, unlike the linear model, nonlinear model shows a significant difference between frequencies of the roof and the long sidewall.

Furthermore, we study the effect of connections on the frequency of vibration using the nonlinear finite element model. The finite element model of the doghouse is also developed to represent connection types A and B. Modeling is performed by deleting the required number of steel frame elements (screws) from the initial finite element model of the doghouse. Modal analysis is performed for the both connection types A and B. Fig. 6.13 shows the first mode of vibration of the long sidewall and the roof for the connection type A. The fundamental frequencies of the long sidewall and the roof are found to be 8.17 Hz and 11.32 Hz respectively.

a) Fundamental mode shape of the wall

Frequency = 8.17481 Hz

b) Fundamental mode shape of the roof

Frequency = 11.32768 Hz

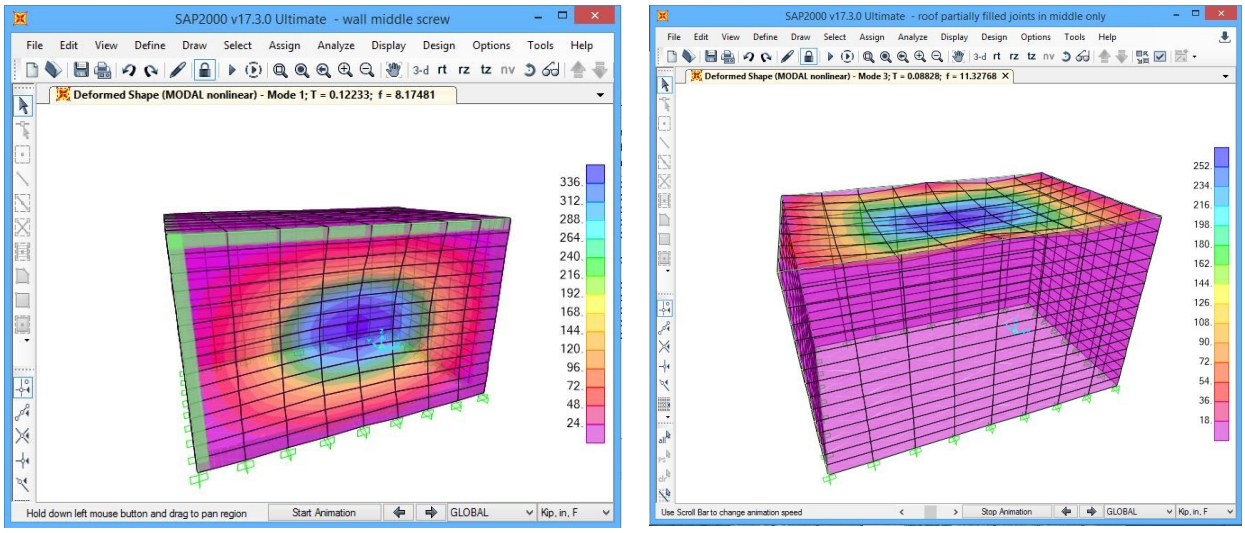

Fig. 6.13. a) Fundamental mode shape and frequency of the long sidewall and b) Fundamental mode shape and frequency of the roof for connection type A, using stress stiffened modes.

Similarly, Fig. 6.14 shows the first mode of vibration of the long sidewall and the roof for the connection type B. The fundamental frequencies of the long sidewall and the roof are found to be 9.44 Hz and 13.83 Hz respectively.

a) Fundamental mode shape of the wall b) Fundamental mode shape of the roof

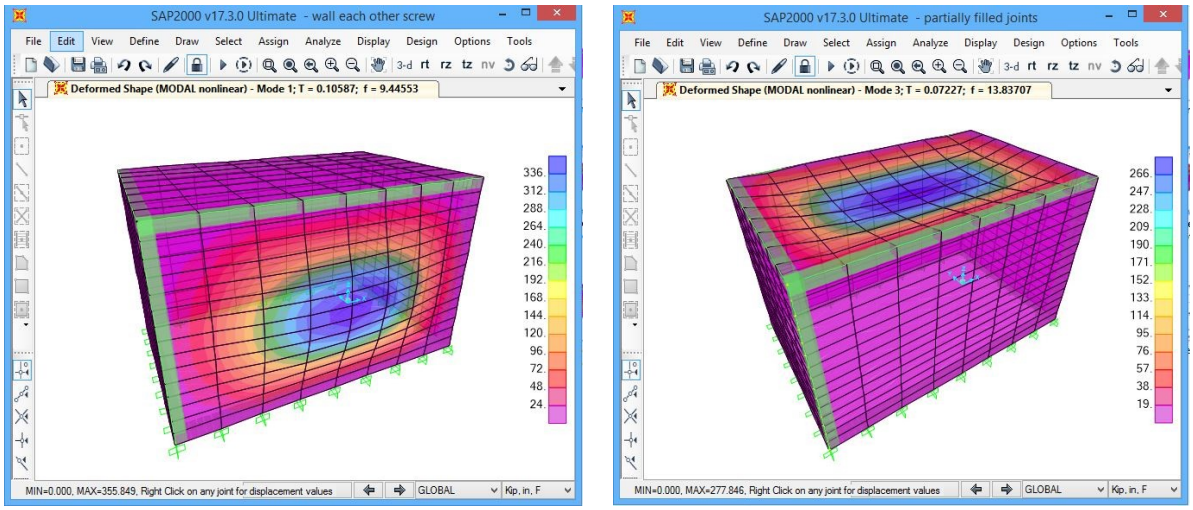

Fig. 6.14. a) Fundamental mode shape and frequency of the long sidewall and b) Fundamental mode shape and frequency of the roof for connection type B, using stress-stiffened modes.

6.6. Summary

We have implemented the linear and nonlinear finite element approach to predict the fundamental frequencies of the roof and the long sidewall of the doghouse. The nonlinear approach predicts fundamental frequencies similar to the experimental test results, while the linear finite element approach does not replicate the experimental results, as shown in Table. 6.1.

Table. 6.1. Comparison between fundamental frequencies of the long sidewall and the roof predicted by linear and nonlinear finite element approach (SAP2000) and experimental tests.

Connection Type/Methods		Linear FEM	Experimental	Nonlinear FEM
A	Wall	8.53 Hz	9.48 Hz	8.17 Hz
	Roof	8.53 Hz	12.6 Hz	11.32 Hz
B	Wall	9.80 Hz	11.07 Hz	9.44 Hz
	Roof	9.80 Hz	13.7 Hz	13.83 Hz
C	Wall	10.36 Hz	11.78 Hz	10.06 Hz
	Roof	10.36 Hz	15.06 Hz	15.45 Hz

Table. 6.1 shows that the linear finite element analysis predicts the same fundamental frequency of the roof and the wall. However, using the nonlinear finite element analysis and experimental tests, we found that the frequency of the roof is significantly higher than that of the long sidewall even if they both have same size, same material, and same boundary conditions. The higher frequency of the roof is due to higher stiffness as a result of large deflection of the roof.

We also found that the frequency varies significantly with respect to number of screw connections. It is obvious that the more restrained is the connection, stiffer is the structure. This is clearly the reason for the increase in fundamental frequency of the roof and the long sidewall in going from connection type A to B to C.

The nonlinear finite element results and the experimental results shown in Table. 6.1 are close but not exact. It might be due to the experimental and numerical errors or we might have to use more sophisticated tools to model nonlinearity, which can be done in future research.

Chapter 7 Identification of Motors Concealed within the Doghouse

This chapter's objectives are to:

- introduce the reader to linear forced vibration analysis of a structure;
- study forced vibration of the doghouse using the finite element model and the experimental tests;
- study the vibration signatures obtained from the doghouse.

7.1. Introduction

We would like study the possibilities of identifying the types, locations and operation of machines concealed within buildings using vibrational information gleaned from the building envelopes. This is a very open-ended problem, which may have no single or optimal solution. However, we think that we can gather valuable information from signals produced by the vibrations of operating machines.

Let us begin with an example. As a fifth-grader, my professor's parents gave him a handsome spring-wound pocket watch for his birthday. He proudly brought that watch to school to show his fellow students, and then placed the watch in his desk, forgetting about it when he went home that day. His teacher heard the tick-tock sound of the watch in the stillness after all the students had left the classroom, and thought there might be a bomb in one of the desks. Clearly, the acoustic signal was sufficient for her to learn something about the watch, concealed out of sight within the desk, although, not enough to know precisely what kind of machine was thus concealed. She gathered this information even without knowing the structural details of the desk.

When gathering vibration from the surfaces of vibrating buildings, one can likewise make guesses about the sources of these observed vibrations. However, we can

say nothing definitive about the source of vibration because multiple sources can produce an identical vibrational signature: for example, a loud speaker can mimic almost any machine from a washing machine to a jet engine to a symphony orchestra. Thus, methods for masking the presence of a machine are readily available which makes the definitive identification of a source almost impossible. In this chapter, we assume that there is no attempt to mask the presence of the postulated concealed machine.

If we know that a building contains a certain type of machine, say, a refrigerator, then we might be able to say the refrigerator is "on" or "off" by listening to the building vibration. We will demonstrate this later in the chapter by performing an experimental test on the doghouse concealing couple of motors in it.

In most of the cases we do not precisely know whether the behavior of the enclosing building is linear or nonlinear. For simplicity, it is reasonable to assume that most buildings vibrate in an approximately linear manner. However, in our case we found that the doghouse showed nonlinear behavior due to stress stiffening effect during the free vibration study. Therefore, in this chapter, we begin by linear analysis, and then perform experimental tests on the doghouse showing nonlinear behavior.

7.2. Linear dynamics

A deterministic system can be described by a function, , that maps an input function, , a function of time , to an output, . Note that both and may be tensors of any order. The essential nature of a linear system is that it satisfies the property of superposition. Given two inputs and to the function, , as well as

their respective outputs and , so that and , then the system is linear if

,

(6.1)

for any scalar values and . The function is called the forcing function, and the function is called the response. If the forcing function and the system function, are given, can be determined.

For example, in the classical problem of linear structural dynamics, one provides a forcing function, , and a system, , and seeks the system state, . To be even more specific, consider the structural dynamics problem, in which a linear building system is known, an earthquake is postulated (based upon seismic data previously obtained), and the deformed state of the building is sought. From the deformed state of the building the structural engineer decides whether or not the building behaves adequately.

In this chapter, our problem is different than the above example. We record a subset of the building vibrations, , we have an approximation of the system function , that is the behavior of the doghouse, and we seek to determine the forcing function of the concealed machinery. Clearly, we can determine certain things about the forcing function, even if we cannot definitely characterize the forcing function and the machine that produces this forcing function.

7.3. Linear forced vibration analysis

A linear structural system can be first discretized using finite elements, and then represented by its mass matrix , its damping matrix , and its stiffness matrix . The linear system equation is thus approximated as the set of second order linear ordinary differential equation

, (6.2)

where is the displacement vector, and is the forcing function. In this form Equation 6.2 requires simultaneous solution of N equations with N unknowns. However, this set of coupled equations can be transformed into a set of uncoupled equations through use of the normal modes of the undamped system (Craig and Kurdila 2006).

Let us consider a single mode. This mode can be thought of as a damped spring mass system, as shown in Fig. 7.1.

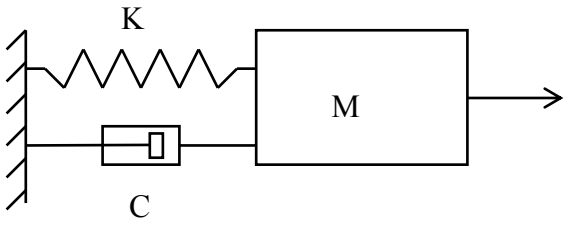

Fig. 7.1. Damped spring mass system.

The system equation for the single degree of freedom system, representing one mode of a multi-degree-of-freedom system, depicted in Fig. 7.1, is

. (6.3)

If we assume harmonic loading with a forcing frequency , , which is a reasonable assumption for a rotating piece of machinery, then the solution is obtained in closed form as a convolution integral:

, (6.4)

where is the system's impulse function, defined as

, (6.5)

where , , and . In addition, the system has a frequency response function, , such that

, (6.6)

where is the periodic forcing function and is the displacement response in the frequency domain. The frequency response function is given by

. (6.7)

Thus, if the acceleration of the single degree of freedom system shown in Fig. 7.1 can be measured, then if system Equation (6.2) is known, the periodic forcing function can be determined. This is a classical linear structural dynamics theory however; we use finite element method (SAP2000) to obtain the response for a given periodic forcing function.

The most important consequence of this derivation is that for a linear system, the periodic displacement response function is proportional to the corresponding periodic input forcing function. Thus, the frequency of the measured periodic acceleration at any point on a linear structure is equal to the frequency of the input periodic forcing function. Linearity also mandates that if there are multiple frequency components to the forcing function, then there will be multiple frequency components on the response function.

7.3.1 Linear finite element analysis

Perhaps the easiest way to demonstrate the linear forced vibration theory explained above is to simply perform a linear time history simulation. A finite element method SAP2000, and the doghouse is used as a system to perform a linear time history simulation.

We have assumed that harmonic loading with a forcing frequency ,

, is a reasonable assumption for a rotating piece of machinery. In the time history simulation, we take as a unit load and is represented by a waveform of frequency of 4.99 Hz, as shown in Fig. 7.2. However, it is not a pure sinusoidal waveform, it is noisy. To make the problem more practical, the experimentally measured waveform including noise is used. This waveform is the time history of a rotating motor measured by the accelerometer in the laboratory.

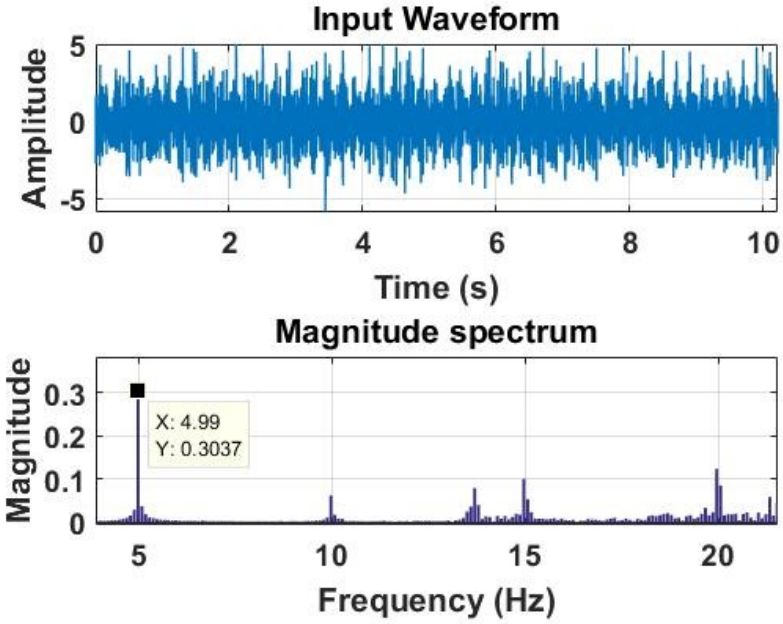

Fig. 7.2. Time history and magnitude spectrum of the input waveform measured in laboratory used for the time history simulation.

A unit force with the given waveform is applied on the doghouse model. The SAP2000 model of the doghouse for time history analysis is shown in Fig. 7.3.

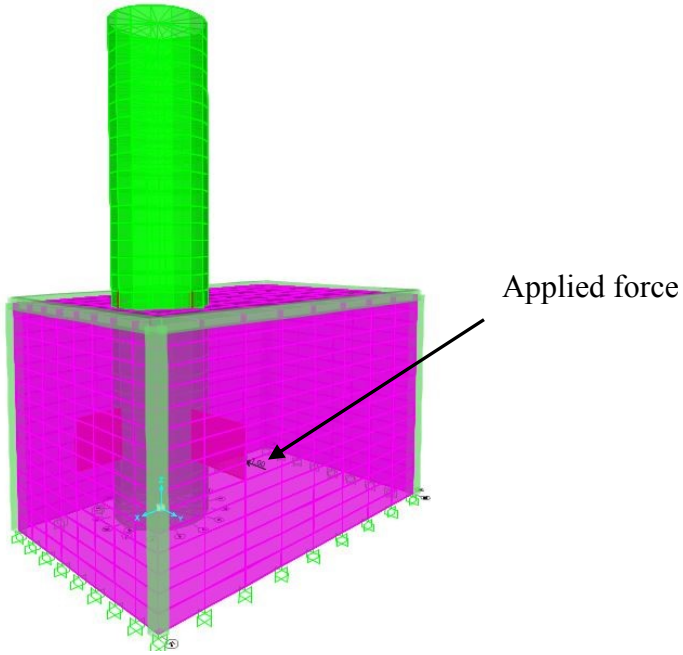

Fig. 7.3. SAP2000 model of the doghouse with the applied force to perform time history analysis.

The periodic force is applied at the junction of the connecting plate and the long sidewall, as shown in Fig. 7.3. Linear time history analysis is performed and a node at the top of the chimney is selected for the displacement output. The displacement time history output of selected joint in the X direction is processed with MATLAB using Discrete Fourier Transform (DFT) to produce frequency of the displacement time history, as shown in Fig. 7.4.

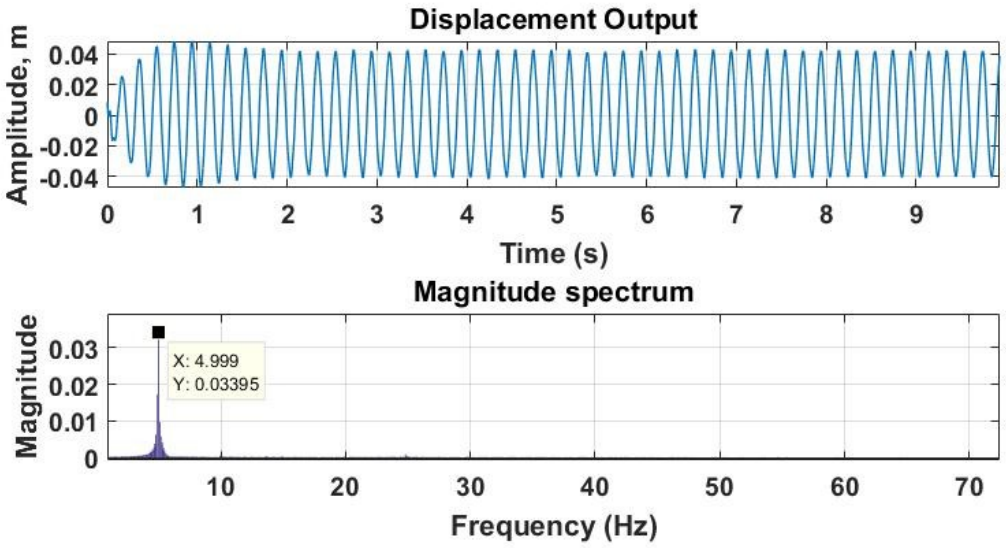

Fig. 7.4. Displacement time history and frequency output at the top of the chimney obtained from linear time history analysis for an input from Fig. 7.2.

It shows that the frequency of the displacement is same as the forcing frequency. Hence, if the system is linear, we can obtain the vibration signature with the same frequency as the forcing function. This demonstrates the linear vibration theory explained in section 6.3. However, our structure shows geometrically nonlinear behavior. Thus, in the next section, we perform the experimental tests on the doghouse to study the relation between the vibration response and the forcing function.

7.4. Laboratory tests of the doghouse

In this section, we would like to study the relation between the periodic input forcing frequency and periodic output response frequency and thus determine to what extent we can characterize the machines concealed within the doghouse using the vibration signatures gleaned from the chimney. Two motors driving off-balance weights are firmly attached to the plate connectors, as shown in following picture in Fig. 7.5. We assume that the reader is already familiar with the geometry of the doghouse from previous chapters. Thus, a portion of the doghouse where the two motors are connected is only shown in the Fig. 7.5.

Fig. 7.5. Picture showing two motors firmly attached with the connecting plates and concealed within the doghouse.

For simplicity, we would like to name the motors. The motor attached with the plate connector connecting chimney and long sidewall is termed as Motor 1, and the motor

attached with the plate connector connecting chimney and short sidewall is termed as Motor 2. These motors are operated by a manual speed controller and we already know the operating frequencies of these motors. Frequencies of Motor 1 and Motor 2 are 4.99 Hz and 7.328 Hz.

Vibration of the chimney is recorded for three different categories, depending upon the operation of the motors. First, Motor 1 is turned on and Motor 2 is turned off. Second, Motor 1 is turned off and Motor 2 is turned on, and third both the motors are turned on. Vibration at the top of the chimney is recorded by the accelerometer as done during free vibration study in Chapter 5 and it is processed with MATLAB using DFT to produce frequency of vibration. Fig. 7.6 shows the vibration signature obtained from the chimney when only the Motor 1 is turned on.

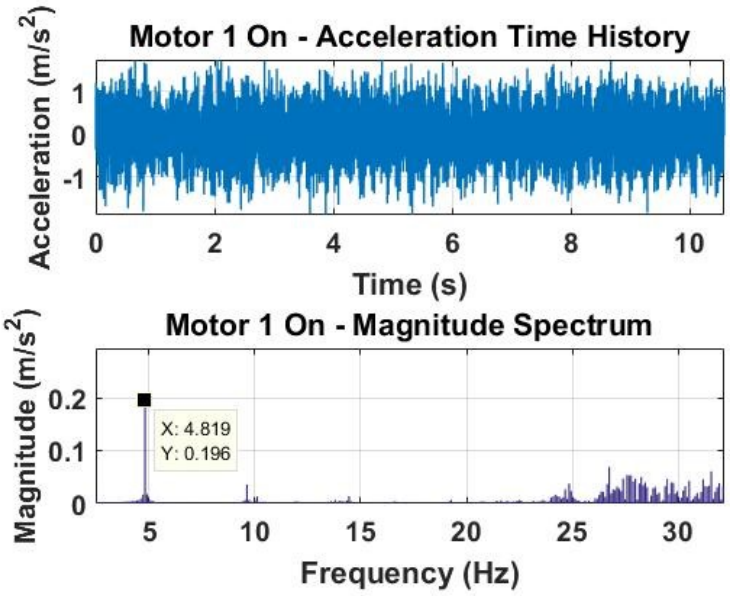

Fig. 7.6. Time history and magnitude spectrum recorded at the chimney when only Motor 1 is turned on.

As can be observed, vibration signature of 4.819 Hz is quite close to the frequency of Motor 1, 4.99 Hz. However, response at frequencies other than the forcing

frequency are also obtained. It might be due to nonlinear behavior of the doghouse, noise during the experiment, and error while processing the data on DFT. Similarly, Figs. 7.7 and 7.8 show the vibration signatures obtained from the chimney when only the Motor 2 is turned on and both the motors are turned on respectively.

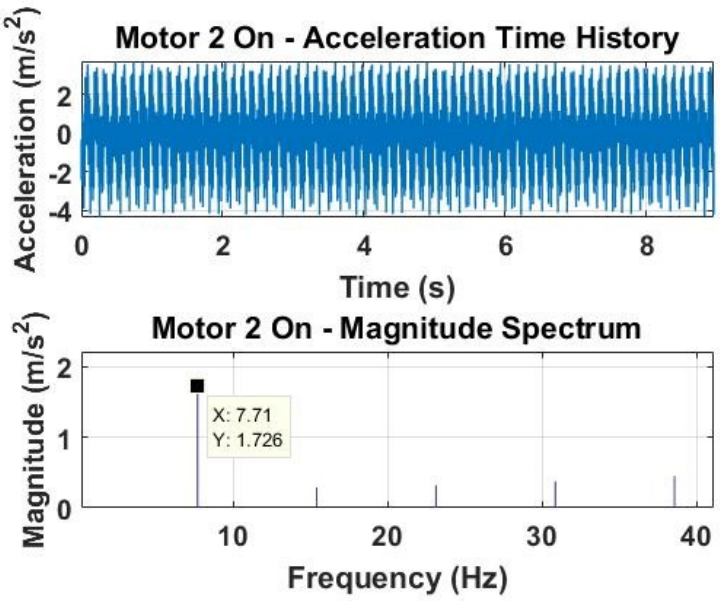

Fig. 7.7. Time history and magnitude spectrum recorded at the chimney when only Motor 2 is turned on.

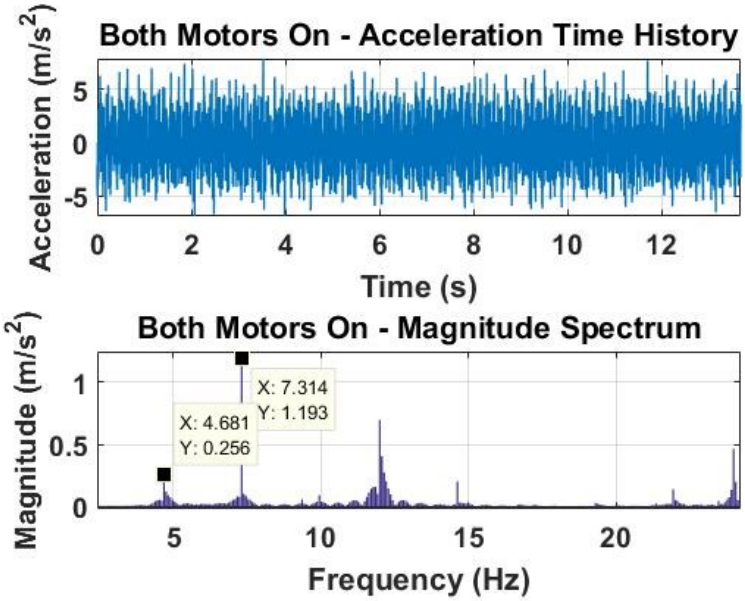

Fig. 7.8. Time history and magnitude spectrum recorded at the chimney when both motors are turned on.

Fig. 7.7 shows the vibration signature of 7.71 Hz is quite close to the frequency of the Motor 2, 7.372 Hz. Similarly, Fig. 7.8 shows the vibration signatures of 4.681 Hz and 7.314 Hz are close to the frequencies of Motor 1 and Motor 2. It shows that, although vibration recorded at the chimney contains various range of frequencies, signatures of the forcing frequencies are always present.

7.5. Summary

In this chapter, we have outlined the background on linear forced vibration analysis and also performed experimental test on the doghouse which has nonlinearity due to stress stiffening effect. We used the finite element method and the experimental tests to study the relationship between periodic input force and periodic output response. Linear time history analysis and experimental tests on the doghouse show that, it is possible to obtain the response with the same frequency as that of forcing function despite the system is linear or nonlinear.

We also studied, to what extent we can characterize the motors concealed within the doghouse by observing the vibrational signatures gleaned from the chimney of the doghouse. Experiments on the doghouse clearly shows that the vibrational signatures recorded at the chimney contains the frequency of the motor causing the vibration. Thus, it is possible to predict whether Motor 1 and Motor 2 are “on” or “off” by observing the vibration signatures obtained from the chimney, although we cannot completely characterize the motors, for example locations and types.

Chapter 8 Vibration Study of the Ford Utility Center

This chapter's objectives are to:

- familiarize the reader to Ford Utility Center;
- study the vibration signatures obtained from the roof of Ford Utility Center;
- determine if there is any correlation between the vibration signatures obtained at the roof and the operation of machinery concealed within the Ford Utility Center.

8.1. Introduction

We have studied the vibration signatures obtained at the chimney due to the concealed motors within the doghouse in Chapter 7. The study showed that by observing the vibration signatures obtained at the chimney, although we cannot definitively characterize the concealed motors within the doghouse, we are able to identify whether the motors are turned on or off.

In this chapter, we would like to extend our study to a more complex existing industrial building to determine whether it is possible to correlate the vibration signatures obtained from the roof of the building with the operation of the machines concealed in it. The Ford Utility Center at the University of New Mexico has been selected to perform this study.

8.2. Ford Utility Center

The Ford Utility Center is a two-story power generating plant located at the premises of the University of New Mexico. It was built on 1948 and the older plant has been expanded and upgraded throughout the years. The Ford plant generation equipment basically includes two natural gas fired combustion turbine generators, a pressure reducing steam turbine generator, two electrically driven centrifugal chillers, and two natural gas fired steam boilers. The site plan, first floor plan and the equipment layout of the Ford Utility Center are shown in Figs 8.1-8.3.

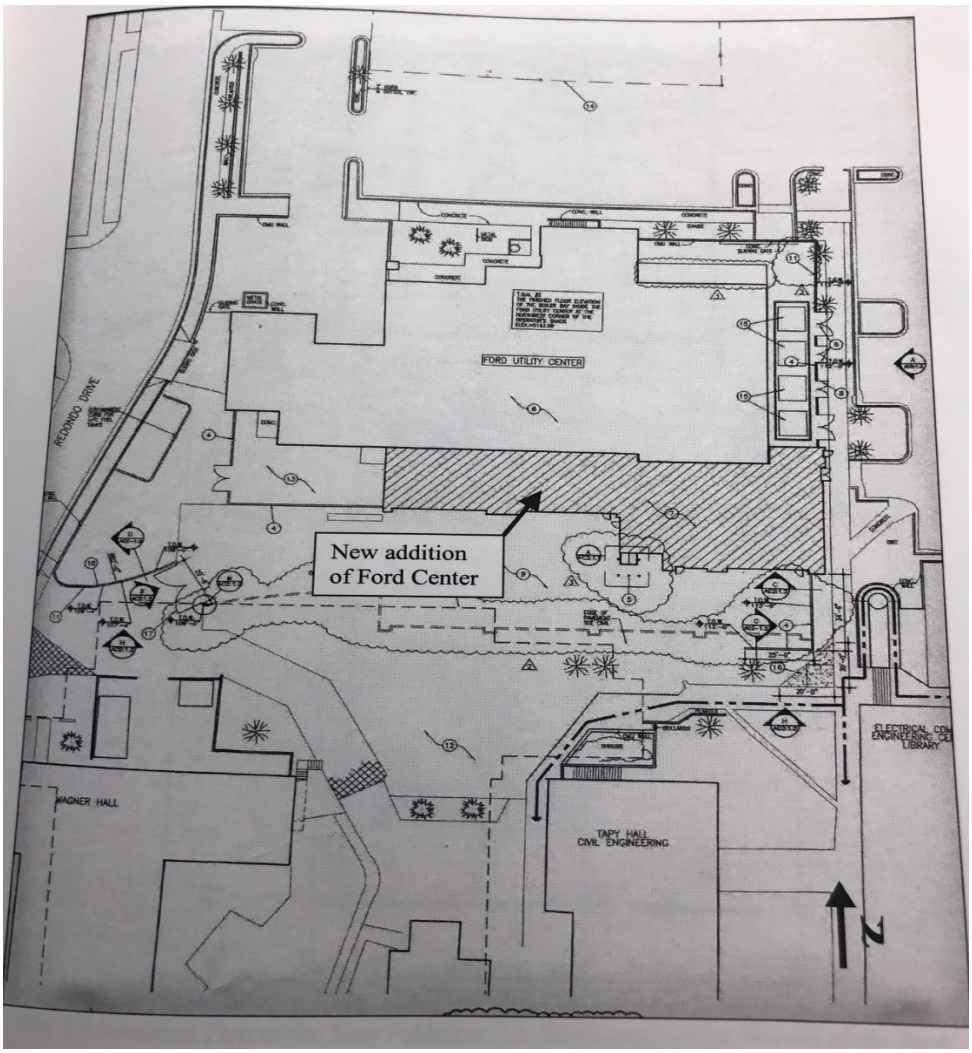

Fig. 8.1. Site plan of Ford Utility Center (Mareddy 2006).

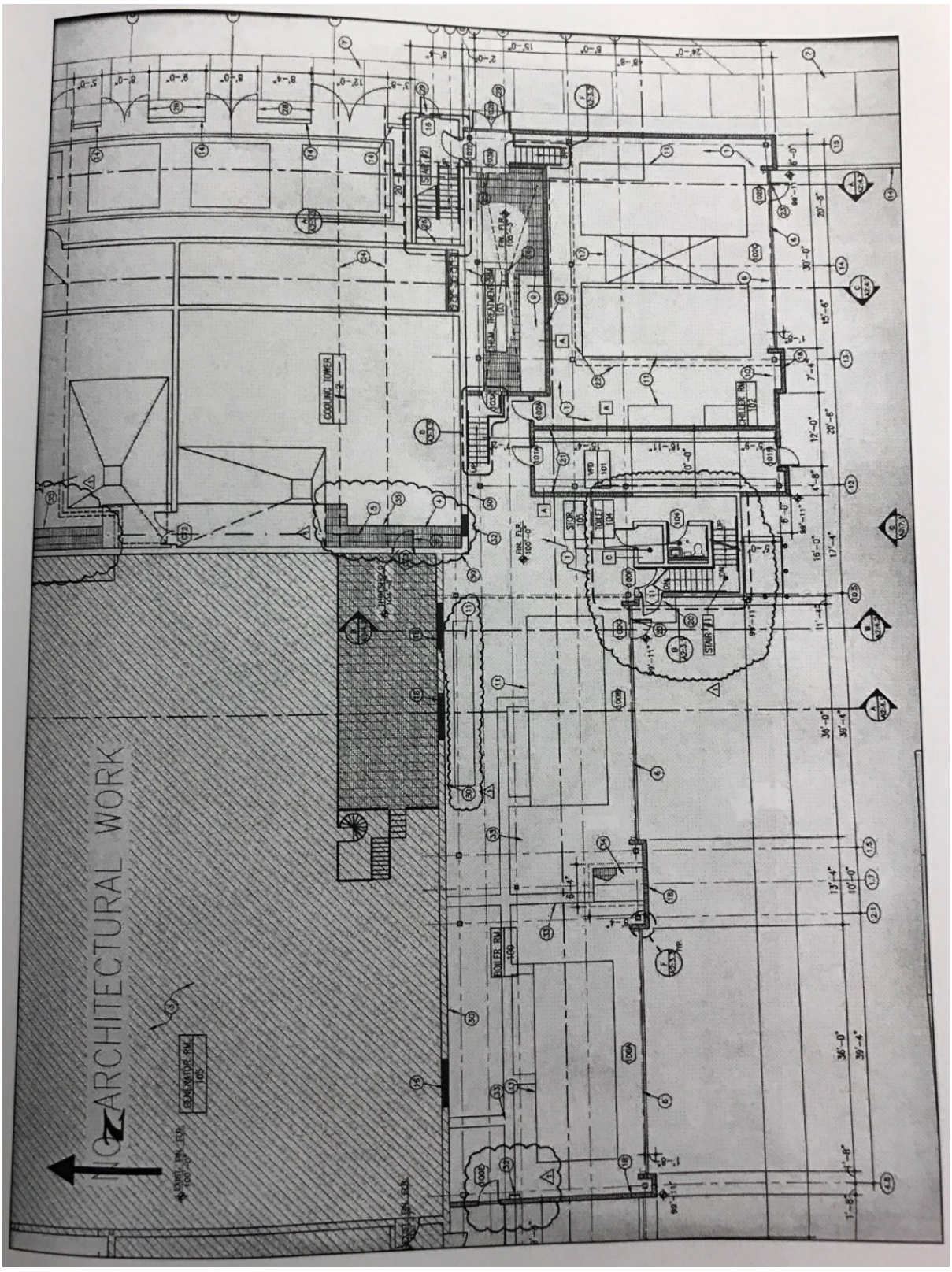

Fig. 8.2. First floor plan of Ford Utility Center (Mareddy 2006).

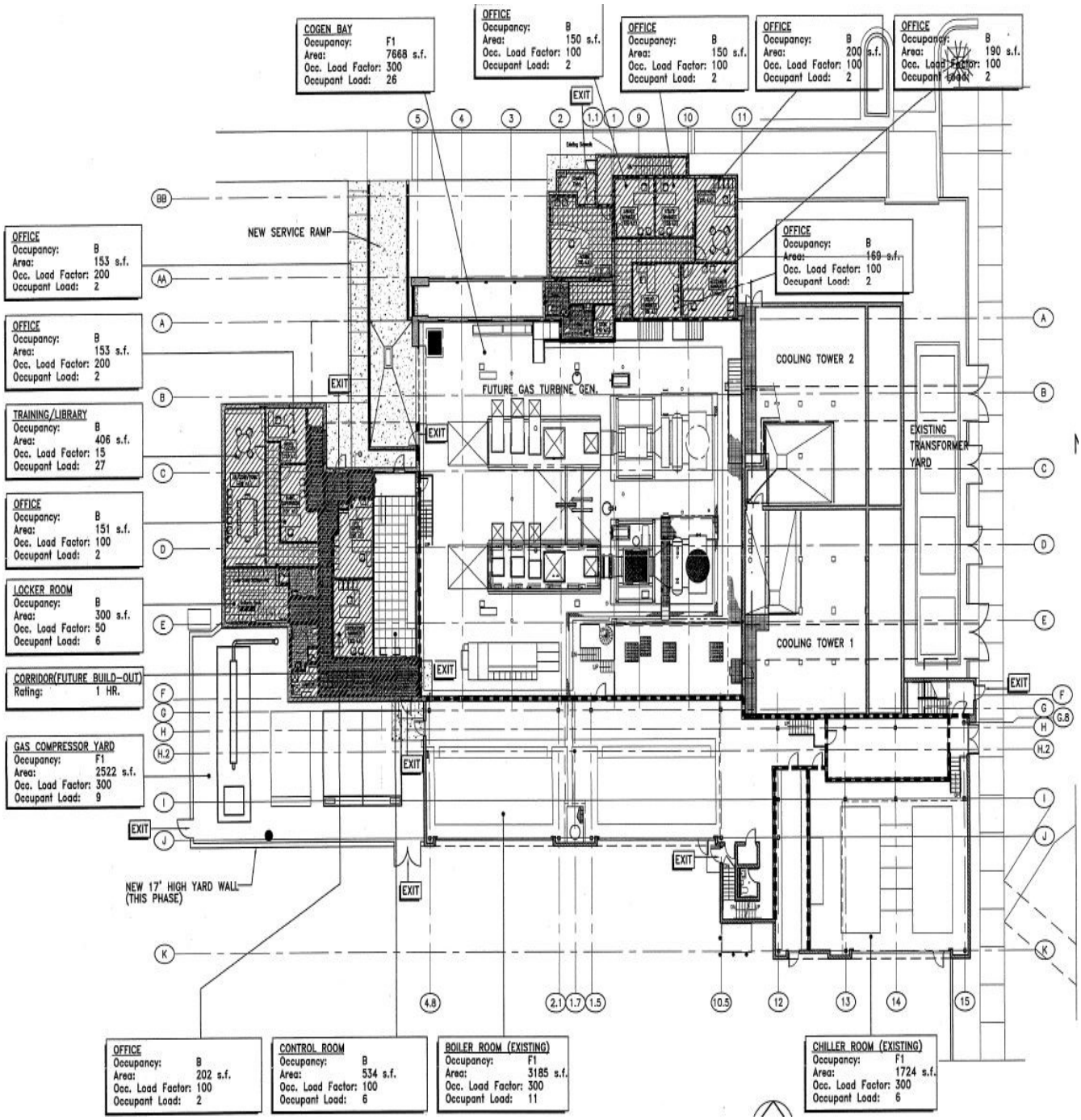

Fig. 8.3. Equipment layout of Ford Utility Center.

The gas turbines, generators and Heat Recovery Steam Generators (HRSG) works mutually to produce electric power and steam and they are collectively called "cogeneration plant". There are two such cogeneration plants within the Ford Utility Center, Cogen 1 and Cogen 2. The gas turbines and generators operate at the speed of 15158 RPM and 1800 RPM respectively. Fig. 8.4 shows the pictures of the two cogeneration plants. The layout of Cogen 1 and Cogen 2 are also shown in the equipment layout plan in Fig. 8.3.

a) Cogen 1 b) Cogen 2

Fig. 8.4. Picture of two Cogeneration plants within Ford Utility Center.

Cogen 1 produces 6.5 MW and Cogen 2 produces 7 MW of power. These are the major machines in the Ford Utility Center which produce the major part of the building vibration. Thus in the next section we mainly try to correlate the operation of these two machine with the vibration signatures taken from the roof of the Ford Utility Center.

8.3. Vibration signatures of the roof

In this section, we record the vibration signatures taken from the roof of the Ford Utility Center. To correlate the vibration signatures recorded on the roof with the

operation of Cogen 1 and Cogen 2, we record vibrations when both the cogeneration plants are operating and one of them is turned off. Since Ford Utility Center must supply utilities to the university continuously, it cannot turn off or on the cogeneration plants according to our experimental requirements. However, due to low demand of energy and water, Cogen 1 is shut down during the weekends. Thus, we record the vibration during the weekdays and weekend to try to correlate roof vibration signatures with machine operations.

Vibration is recorded at the air outlets of Cogen 1 and Cogen 2 located on the roof of Ford Utility Center. Fig. 8.5 shows a Google image of the roof of the Ford Utility Center and the two circles highlight the air outlets of Cogen 1 and Cogen 2, which we term as Location 1 and Location 2, respectively.

Fig. 8.5. Google image of the roof of Ford Utility Center.

The vibration of Location 1 and Location 2 are recorded on three different dates, April 1st 2016 (Friday), April 2nd 2016 (Saturday), and April 8th 2016 (Friday). The machinery operating under the Ford roof on these dates are shown in Table 8.1.

Table. 8.1. Machinery operating in the Ford Utility Center on the given three dates.

Machines	April 1st 2016 (Friday)	April 2nd 2016 (Saturday)	April 8th 2016 (Friday)
Cogen 1	On	Off	On
Cogen 2	On	On	On
Steam Turbine	On	On	On
East Chiller	Off	Off	Off
West Chiller	Off	Off	Off
East Boiler	Off	Off	Off
West Boiler	Off	Off	Off

As shown in Table 8.1, other than Cogen 1 is turned off on Saturday April 2nd 2016, all the other machines have the same operating status on all three dates.

The measured vibration data are logged and the corresponding discrete Fourier Transform magnitude spectra are computed. Fig. 8.6 shows the magnitude spectra of vibration measured at Location 1 on the three dates.

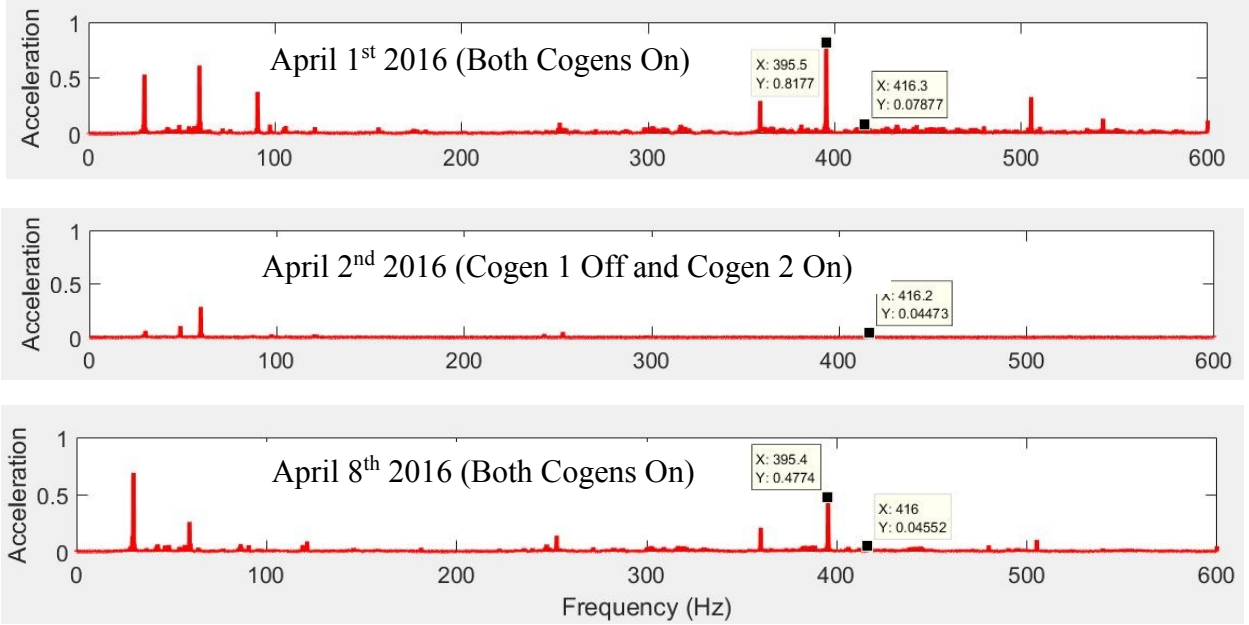

Fig. 8.6. Magnitude spectra of the vibrations measured at Location 1 on three dates.

As can be observed, we obtained various frequency spectra on the three dates. However, peaks at approximately 395.5 Hz and 416.3 Hz are highlighted in Fig. 8.6. According to Fig. 8.6, on April 1th and 8th when both of the cogeneration plants are operating, both the peaks at frequencies 395.5 Hz and 416.3 Hz appeared on the magnitude spectra but, on April 2nd when the Cogen 1 is turned off, the peak at 395.5 Hz disappears. Fig. 8.6 also shows that the amplitude at 395.5 Hz is higher than the amplitude at 416.3 Hz.

Fig. 8.7 presents the magnitude spectrum of vibration recorded at the Location 2 on the same three dates. Similar to the magnitude spectra in Fig. 8.6, Fig. 8.7 also shows that the peaks at 395.5 Hz and 416.3 Hz appear on the magnitude spectra when both the cogeneration plants are in operation and the peak at frequency 395.5 Hz disappears when the Cogen 1 is turned off. It also shows that the amplitude at 416.3 Hz is higher than the amplitude at 395.5 Hz.

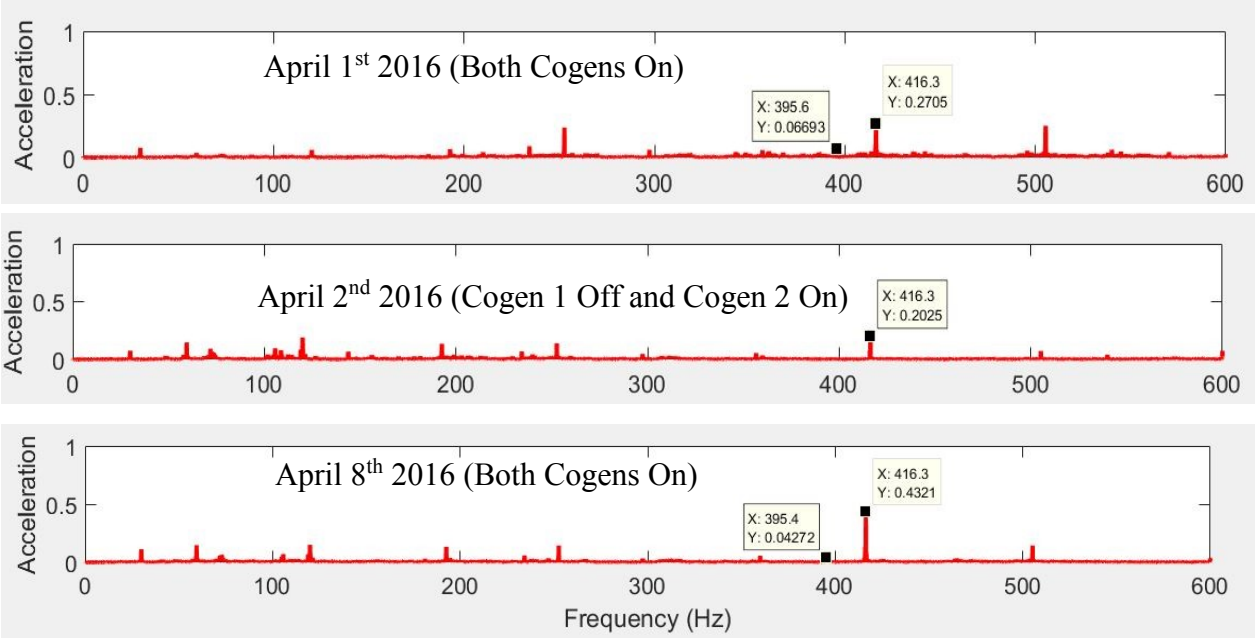

Fig. 8.7. Magnitude spectra of the vibrations measured at the Location 2 on three dates.

The magnitude spectra of vibrations measured at Location 1 has a dominant peak at 395.5 Hz and the dominant peak of Location 2 is at 416.3 Hz. Moreover, the peak at 395.5 Hz disappears on the magnitude spectra of both locations when Cogen 1 is turned off. We infer that the vibration signatures of 395.5 Hz and 416.3 Hz are produced by the Cogen 1 and Cogen 2, respectively.

Additionally, apart from the vibration signatures of 395.5 Hz and 416.3 Hz there are noticeable peaks at many other frequencies. Although we have presented the vibration data recorded only at the air outlets of the cogeneration plants, in fact we recorded vibration data from many different locations on the roof of the Ford Utility Center. In most of all data, including the records presented in this section, we found the common vibration signatures of 30 Hz and 60 Hz on all the magnitude spectra. However, the amplitudes varied depending on the operation of cogeneration plants and the location of the data measurements. According to the operators at the Ford Utility Center, the

generators and electrical power supplied by the Ford utility Center is at 60 Hz and there are no machines that operates at the frequency of 30 Hz. Therefore, the frequency of 60 Hz might be the signature of the electrical power supplied by the Ford Utility Center and the 30 Hz might be the natural frequency some mode of vibration of the roof. Other high frequency peaks on the magnitude spectrum may be due to various types of machinery and vibrating ducts and piping.

8.4. Summary

In this chapter, we have presented the vibration study of a real industrial building, the Ford Utility Center. The results of this study show that by studying the vibration signatures recorded at the air outlets of the cogeneration plants on the roof, it is possible to predict whether the cogeneration plants are operating or not.

In general, machinery produces a pattern of vibration on the roof. The main problem is that in a building like the Ford Utility Center, it is almost impossible to obtain a clean sinusoidal vibration from the roof of the building. In noisy data, machine signatures might be hidden in the noise from other sources. Thus, one has to know what to look for. For example, the magnitude spectra of vibrations recorded at Location 1 and Location 2 contain various ranges of frequencies out of which 395.5 Hz and 416.3 Hz are the ones which correlates with the operation of the cogeneration plants concealed within the building.

Chapter 9 Conclusions

This chapter's objectives are to:

- summarize this thesis;
- draw conclusions;
- suggest future research in this field.

9.1. Summary

In this thesis, we studied the possibility of identifying the operation of machines concealed within buildings using vibrational information gleaned from the building envelopes. It was a challenging task in general because for the same source of input, vibrational signatures recorded from the building envelopes may be altered by the building's details. Also, multiple mechanical sources can produce identical vibration signatures. For example, a loud speaker can mimic almost any machine, from a washing machine to a jet engine. We began with a brief review of the previous work performed by a former graduate student and team members of this research project, emphasizing their findings and weaknesses. We studied data acquisition process, acceleration time history, and the displacement time histories of vibrations in the preliminary stage of our research.

The final task of our research was to study the vibration of the roof and the exhaust structures of the Ford Utility Center due to the concealed machinery within it. For this, we decided first to simulate the problem using a simple laboratory structure. We built a simple laboratory structure called the "doghouse" representing an industrial building like the Ford Utility Center. A free vibration study of the doghouse using the linear finite element model and experimental test showed the linear finite element model

was inadequate to model the vibration behavior of the doghouse. We then refined our laboratory structure and included geometric nonlinearity due to large displacement in the finite element model. The finding justified that the doghouse is geometrically nonlinear due to the stress stiffening effect of gravity. We also studied the effect of connections on the vibration of the doghouse using the finite element model and the experimental test. We found that there was a significant change in frequency of vibration of the doghouse when the screws were loosened and tightened.

We then studied the vibration signatures of the chimney of the doghouse caused by two motors operating within it. By observing the vibration signatures of the chimney, we were able to determine whether one of the motors inside the doghouse is turned on or off. This controlled experiment using the doghouse provided better understanding to enable us to predict the operation of the machinery concealed within the Ford Utility Center.

Finally, we presented the vibrational study of the Ford Utility Center. We found that, although the vibration signatures of the exhausts structures at the roof were very noisy, interestingly, by pattern recognition, we were able to determine whether the cogeneration plants concealed within the building were operating or not.

9.2. Major findings

By performing the free vibration study of the doghouse using a finite element model (SAP2000) and an experimental test, as expected in a real structure, we found the doghouse demonstrated a degree of nonlinearity. Thus, one should be always careful in simplifying a real-world problem in assuming it to be linear elastic.

We also found that structural vibrations are sensitive to minor details. For example, we found there was a significant change in frequency of vibration of the doghouse when the screws were loosened or tightened. It is not easy to model an existing complex industrial building by including all the details such as connections, supports, dampers, and insulations. However, a finite element model created with simplifying assumptions nevertheless provides valuable information about the structural behavior. Thus, we conclude pattern recognition method appears to be a good way to detect concealed machines, in collaboration with model-based simulation approaches.

The research was focused on answering the question: "By measuring the vibration signatures on the roof of a building, is it possible to identify the types, locations and the operation of machines causing vibration?" From the vibration study of the doghouse and the Ford Utility Center, Figs. 7.6, 7.7, 7.8, 8.6, and 8.7 show that machinery produces a pattern of vibration signatures on the roof and exhaust structures. By using this pattern of vibration signatures, we were able to identify the operation of machinery concealed within the building. However, in this thesis we are not able to identify the types and locations of the concealed machinery by structural simulation. Additionally, the pattern of vibration signatures recorded on the chimney of the doghouse are directly related with the frequencies of the concealed motors, however, the pattern of vibration signatures recorded on the roof of the Ford Utility Center does not relate with the frequencies of cogeneration plants.

9.3. Future research

Due to the inherent assumptions of SAP2000, in this thesis, after taking the nonlinearity due to stress stiffening effect into account, we assumed the vibrations are

linear. Is this realistic? We feel the model can be improved by using more sophisticated nonlinear finite element analysis software like ABAQUS.

All the vibrations recorded on the doghouse and the Ford Utility Center produced noisy data. We used the interesting peaks at certain frequencies to draw conclusions and neglected all the other peaks, calling them noise. How realistic is this? In a nonlinear system, periodic forcing at a given frequency often produces vibrations of the same frequency; however, a nonlinear system also produces periodic responses other than the nominal forcing frequency. Moreover, in a nonlinear system, periodic forcing at a given frequency can also produce chaotic response. Thus, the interpretation of a vibration signal might be improved in future research.

For example, a squeaky wheel on a cart sends a signal that oil is needed, even without further knowledge about the wheel, bearing, or cart. The type of squeaky signal may provide additional information. While only frequency of vibration was considered for identification purpose, however, amplitude of vibration may also contain valuable information to identify the types and locations of vibrating machines, which can be investigated in future research.

References

Allemang, R. J. (1998). "Survey of Nonlinear Detection and Identification Techniques for Experimental Vibrations."

Boothby, T. E., D. E. Domalik and V. A. Dalal (1998). "Service load response of masonry arch bridges." Journal of structural engineering **124**(1): 17-23.

Chang, P. C., A. Flatau and S. Liu (2003). "Review paper: health monitoring of civil infrastructure." Structural health monitoring **2**(3): 257-267.

Craig, R. R. and A. J. Kurdila (2006). Fundamentals of structural dynamics, John Wiley & Sons.

Doebling, S. W., C. R. Farrar, M. B. Prime and D. W. Shevitz (1996). "Damage identification and health monitoring of structural and mechanical systems from changes in their vibration characteristics: a literature review."

Farrar, C. R., K. Worden, M. D. Todd, G. Park, J. Nichols, D. E. Adams, M. T. Bement and K. Farinholt (2007). Nonlinear system identification for damage detection, Los Alamos National Laboratory (LANL), Los Alamos, NM.

Han, S. (2010). "Measuring displacement signal with an accelerometer." Journal of Mechanical Science and Technology **24**(6): 1329-1335.

Han, S. and J. W. Chung (2002). Retrieving displacement signal from measured acceleration signal. Proceedings of 20th International Modal Analysis Conference (IMAC'02).

Lee, H. S., Y. H. Hong and H. W. Park (2010). "Design of an FIR filter for the displacement reconstruction using measured acceleration in low frequency dominant structures." International Journal for Numerical Methods in Engineering **82**(4): 403-434.

Leissa, A. W. (1969). Vibration of plates, DTIC Document.

Levy, S. (1942). Bending of rectangular plates with large deflections, DTIC Document.

Love, A. E. H. (1888). "The small free vibrations and deformation of a thin elastic shell." Philosophical Transactions of the Royal Society of London. A **179**: 491-546.

Mareddy, S. (2006). "An analysis of service level vibrations in a utility building."

Moreu, F., H. Jo, J. Li, R. Kim, S. Cho, A. Kimmle, S. Scola, H. Le, B. Spencer Jr and J. LaFave (2014). "Dynamic assessment of timber railroad bridges using displacements." Journal of Bridge Engineering **20**(10): 04014114.

Oppenheim, A. V., A. S. Willsky and S. H. Nawab (1983). Signals and systems, Prentice-Hall Englewood Cliffs, NJ.

Pérez, F., J. B. Campbell, M. Jaramillo, R. Dunkel, T. Atwood, A. Doerry, W. H. Gerstle, B. Santhanam and M. M. Hayat (2016). Exploiting synthetic aperture radar imagery for retrieving vibration signatures of concealed machinery. SPIE Defense+ Security, International Society for Optics and Photonics.

Sathyamoorthy, M. (1987). "Nonlinear vibration analysis of plates: a review and survey of current developments." Applied Mechanics Reviews **40**(11): 1553-1561.

Timoshenko, S. P. and S. Woinowsky-Krieger (1959). Theory of plates and shells, McGraw-hill.

Von Karman, T. (1910). Festigkeitsprobleme im maschinenbau, publisher not identified.